Tutorial Series: Beam Instrumentation and Measurement Challenges

MICHIKO MINTY

NAPAC 2019

3 SEPTEMBER 2019

Beam Instrumentation and Measurement Challenges

- Beam Instrumentation
- Measuring Beam Parameters and Characterizing Accelerator Performance
- Selected Recent Developments and Future Challenges

Beam Current and Beam Power, definitions

Current, I = charge passing a given point per unit time (t) = Q / t = Q f

where Q = total number of particles in the beam = n e V

with n = number of charges per unit volume, V = volume
e = electric charge = 1.6E-19 Coulombs
f = bunch repetition frequency (Hz)

Beam power, P = product of beam current and beam energy / unit charge = I (E/e)

where E = beam energy (in eV)

Duty factors F_i, which determine the bunch structure, are multiplicative:

$$P = Q_b \, f \prod_i F_i \, E/e$$

Note $I = Q_b \, f$

$$\langle I \rangle = Q_b \, f \prod_i F_i$$

where P (W) = beam power
Q_b (C) = charge per bunch
f (Hz) = repetition frequency
and E (eV) = beam energy

Beam Current Measurements – Faraday Cup

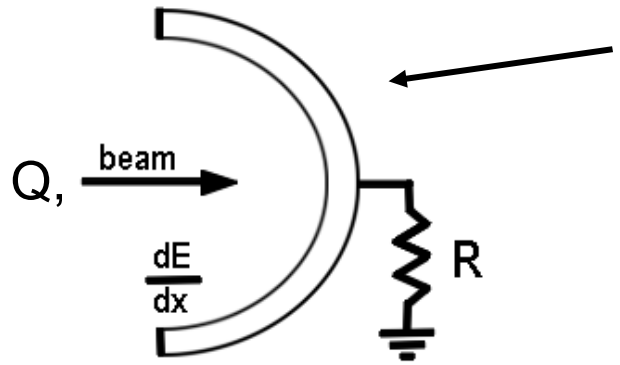

thick (e.g. ~0.4 m copper for 1 GeV electrons) or series of thick (e.g. for cooling) charge collecting conducting receptacles

principle: beam deposits (usually) all energy into the cup (invasive)
charge converted to a corresponding current (I=dQ/dt)
voltage across resistor proportional to instantaneous current absorbed

challenges:

- bandwidth-limited (~1 GHz) due to capacitance to ground
- cooling needed for high power beams
- backscattering (due to electromagnetic showers)
- secondary emission (ionization products) – mitigated by adding a positive bias to cup (or to grid preceding cup) to retain electrons

"Faraday-Cup Monitors for High-Energy Electron Beams", K.L. Brown and G.W. Tautfest, Rev. of Sci. Instr. **27**, 696 (1956)

Photo of an in-flange Faraday cup

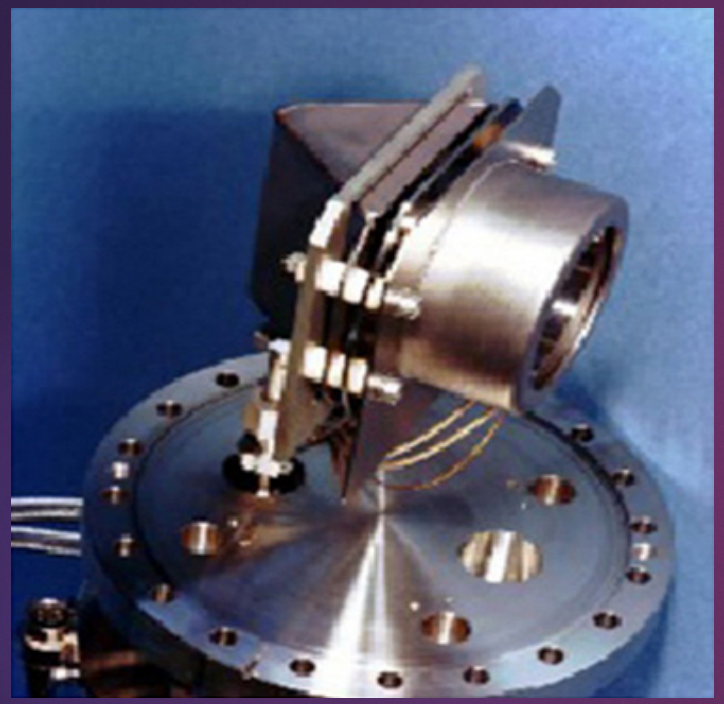

Cup and shield:	Tantalum
Cup support:	Stainless Steel
Cup insulation:	Ceramics
Cup shape:	Conical
Max. beam power:	600 W (uncooled version) / 6 kW (cooled version)
Connector:	BNC
Max. high voltage:	2500 V
UHV-Feedthrough:	Compressed air actuated Feedthrough

cross-sectional sketch of FC (KEKB Injector linac)

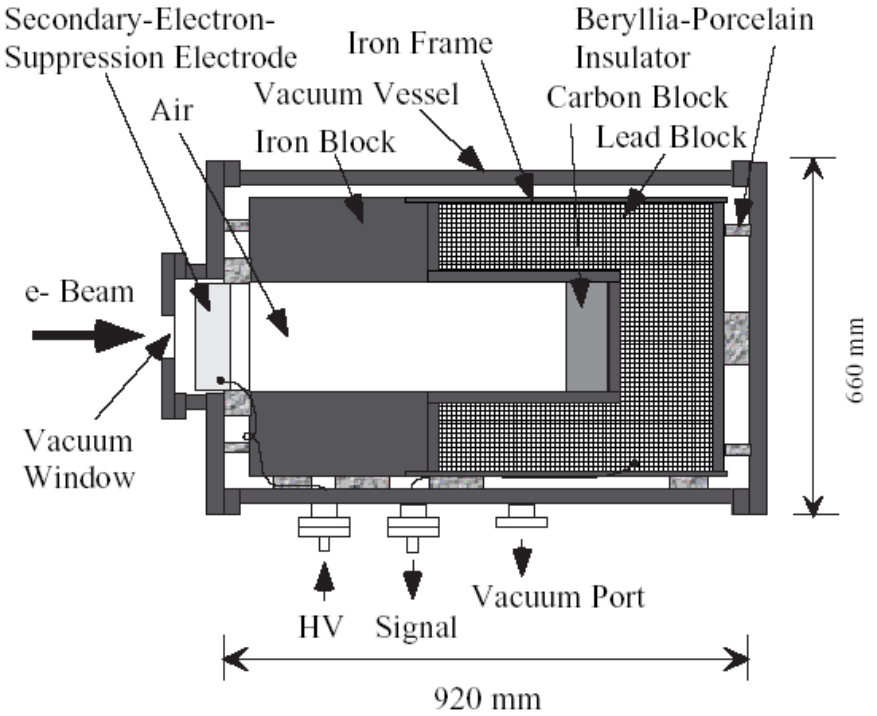

cylindrically symmetric blocks of lead (~35 rad lengths)

carbon and iron - for suppression of “backscattering” / “electro-magnetic showers”; i.e. particles liberated from nuclear reactions generated by the lead)

bias voltage (~many 100 Volts) for suppression of “secondaries”; i.e. electrons generated by Compton scattering

courtesy T. Suwada

Beam Current Measurements – Current Transformer

Consider a magnetic ring surrounding the beam, from Ampere's law:

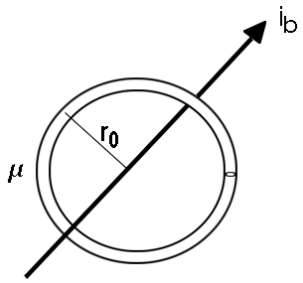

(integral over circumferential length of magnetic core)

$$\oint \vec{B} \cdot \vec{dl} = \mu I$$

μ = permeability of core
= $\mu_r \mu_0$, where μ_r is magnetic permeability of medium
and μ_0=4πe-7 [H/m] is the permeability of free space

if r_0 (ring radius) >> thickness of the toroid, $$B = \frac{\mu i_b}{2\pi r_0}$$

Add an N-turn coil – an emf is induced which acts to oppose B:

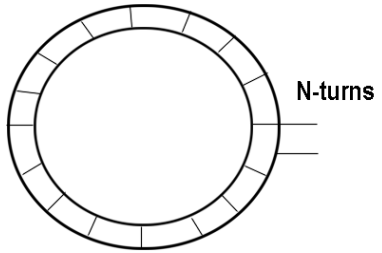

$$\epsilon = \frac{d\phi}{dt} \text{ where } \phi = \int \vec{B} \cdot d\vec{a}$$
$$= \frac{\mu A}{2\pi r_0} \frac{di_b}{dt}$$

A is the cross-sectional area of the magnetic ring

Load the circuit with an impedance; from Lenz's law, $i_R = i_b/N$:

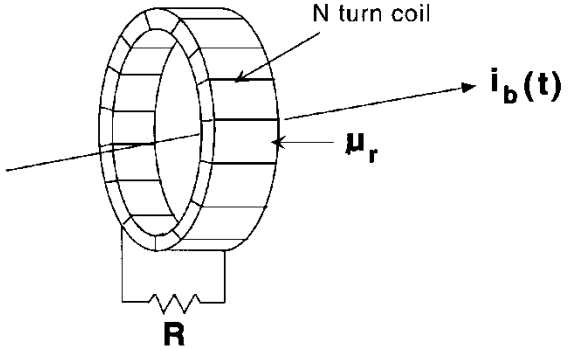

The N-turn coil serves as a primary/secondary winding of a current transformer while the intercepting beam acts as secondary/primary winding.

principle: the combination of core, coil and R produce a current transformer such that i_R (the current through the resistor) is a scaled replica of i_b. This can be viewed across R as a voltage.

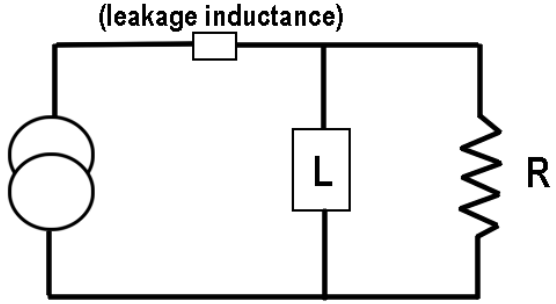

$$L = \frac{N^2}{R_h}$$

with R_h = reluctance of magnetic path

$$R_h = \frac{l}{\mu A}\ [\mathrm{H}^{-1}] \longrightarrow L = \frac{N^2 \mu_r \mu_0 A}{l}$$

sensitivity:

$$S = \frac{R}{\sqrt{1 + (\frac{\omega_l}{\omega})^2}} \qquad \omega_l = \frac{R}{L}$$

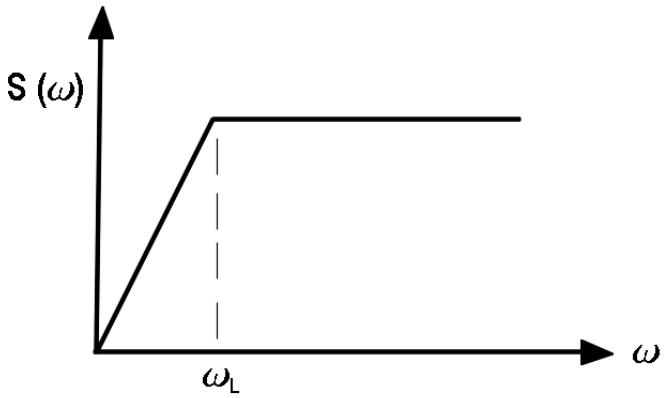

cutoff frequency, ω_L, is small if $L \sim N^2$ is large

detected voltage:

$$V(t) = \frac{i_b R}{N} e^{-(\frac{R}{L})t}$$

if N is large, the voltage detected is small

challenge: trade-off between bandwidth and signal amplitude

Photo of a beam current transformer

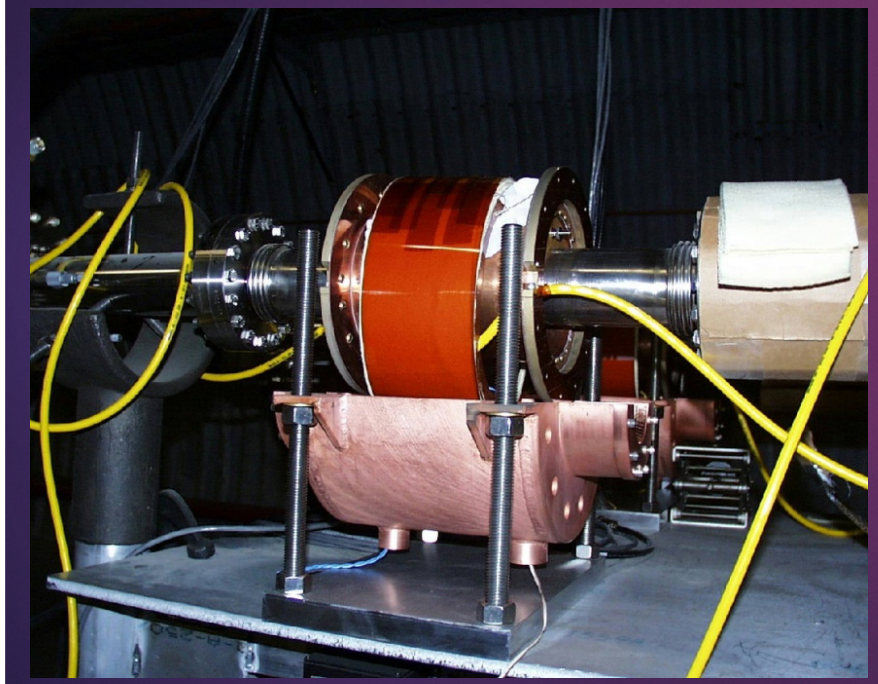

scope trace from measurements (in a transfer line)

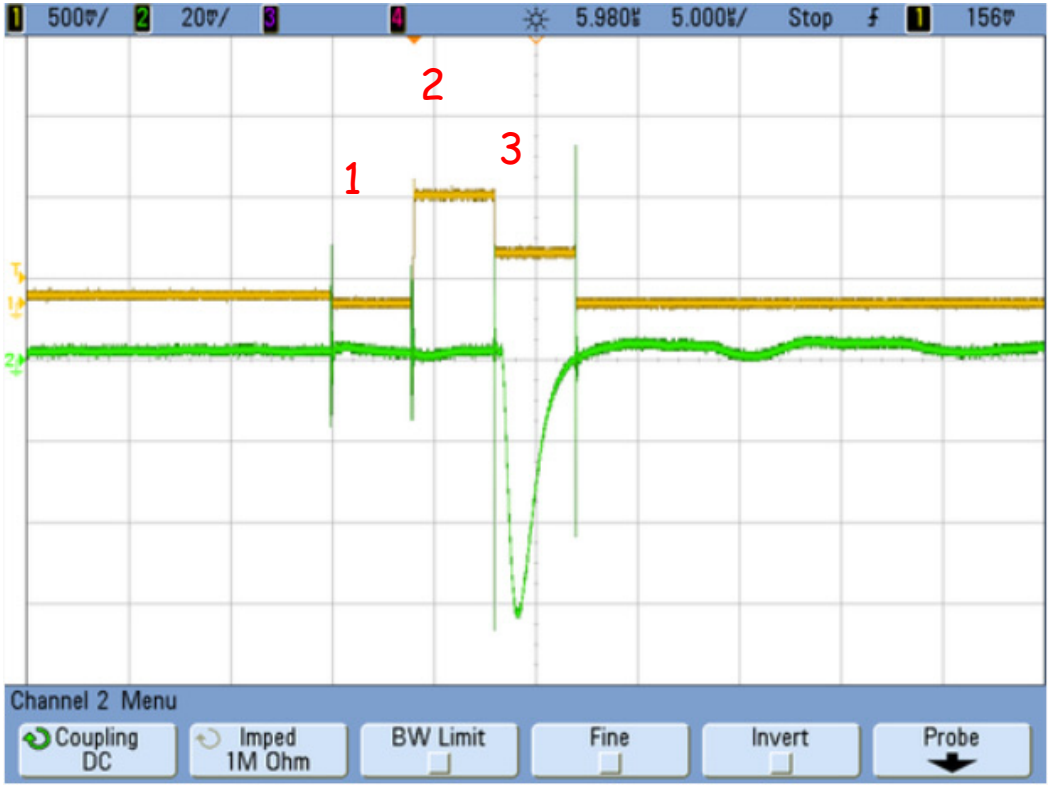

triggering timing

1. baseline clamping
2. integration window for baseline offset and noise
3. integration window for signal of interest

Beam Current Measurements – Wall Current Monitor

Fields of a relativistic particle

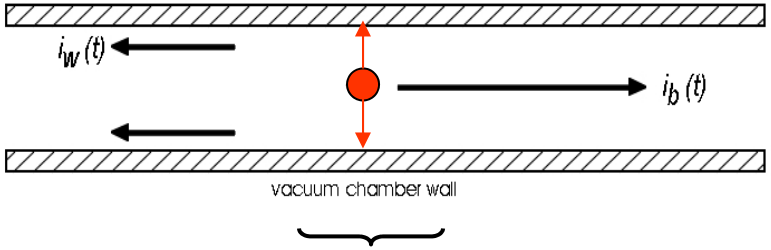

Lorentz-contracted “pancake”

induced wall current $i_w(t)$ has opposite sign of beam current $i_b(t)$: $i_b(t)=-i_w(t)$

Detection of charged particle beams

i_w is a current source

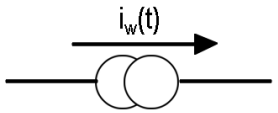

with infinite output impedance, i_w will flow through any impedance placed in its path

many “classical” beam detectors consist of a modification of the walls through which the currents will flow

Wall Current Monitor

principle

remove a portion of the vacuum chamber and replace it with some resistive material of impedance Z

detection of voltage across the impedance gives a direct measurement of beam current since $V = i_w(t)\,Z = -i_b(t)\,Z$

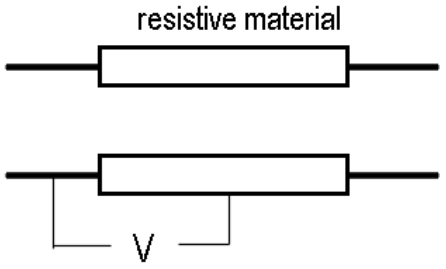

(susceptible to em pickup and to ground loops)

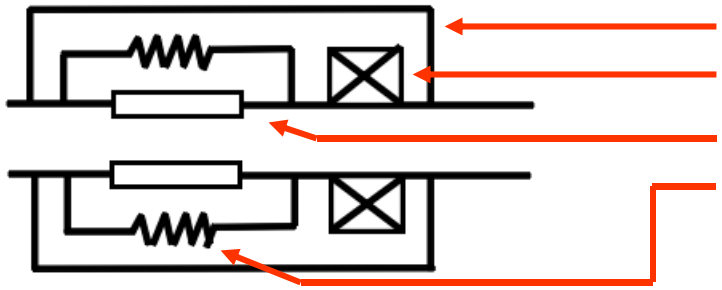

add high-inductance metal shield
add ferrite to increase L
add ceramic breaks
add resistors (across which V is to be measured)

alternate topology - one of the resistors has been replaced by the inner conductor of a coaxial line

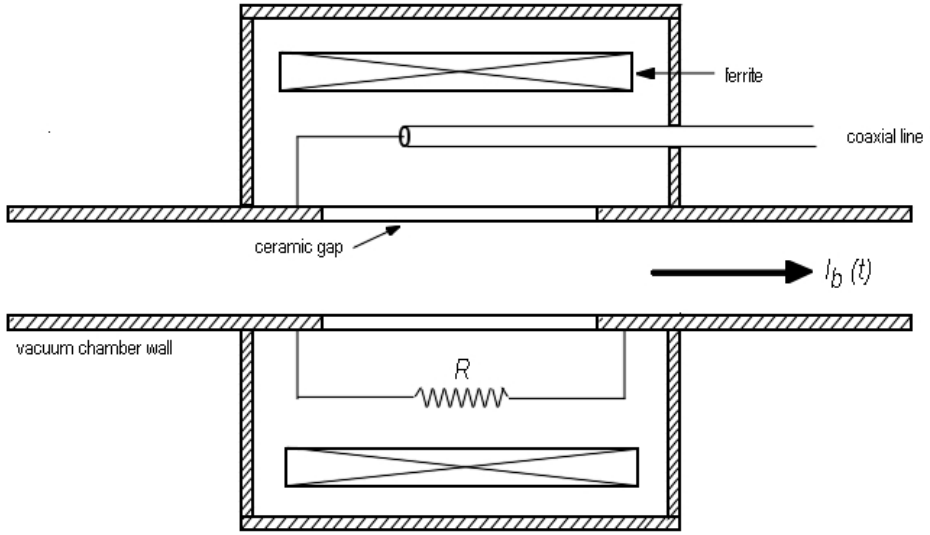

Wall Current Monitor

sensitivity:

circuit model using parallel RLC circuit:

$$\frac{1}{Z} = \frac{1}{R} + \frac{1}{j\omega L} + j\omega C$$

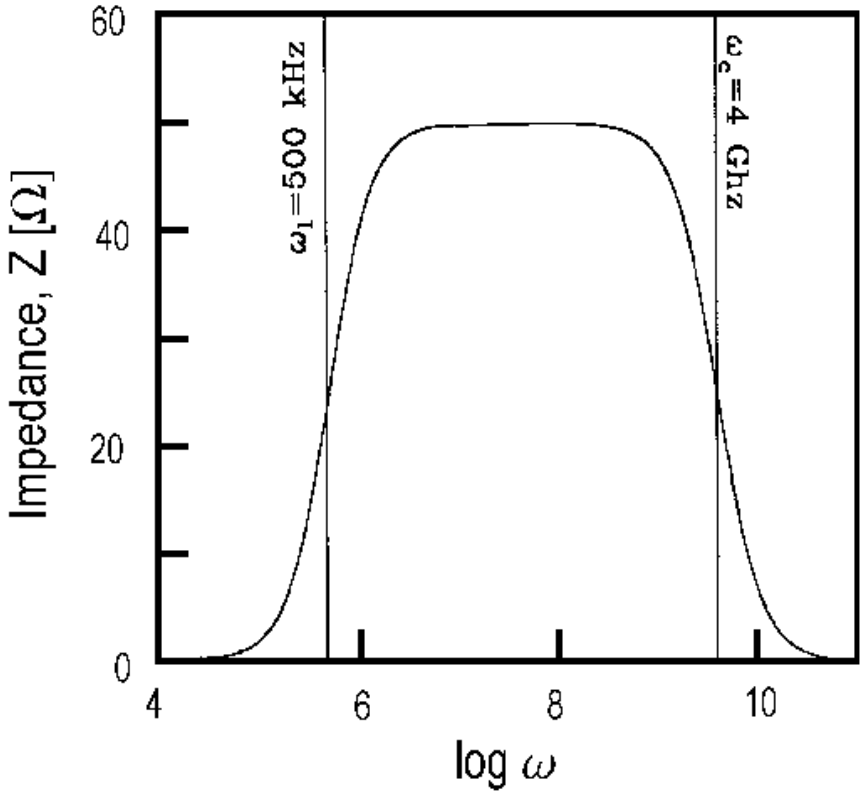

high frequency response is determined by C:

$$|Z(\omega \to \infty)| = \frac{R}{\sqrt{1 + (\frac{\omega}{\omega_C})^2}} \qquad (\omega_C = 1/RC)$$

low frequency response determined by L:

$$|Z(\omega \to 0)| = \frac{R}{\sqrt{1 + (\frac{\omega_L}{\omega})^2}} \qquad (\omega_L = R/L)$$

intermediate regime: $R/L < \omega < 1/RC$ – for high bandwidth, L should be large and C should be small

note: this simplified model does not take into account the fact that the shield may act as a resonant cavity

Photo of a wall current monitor

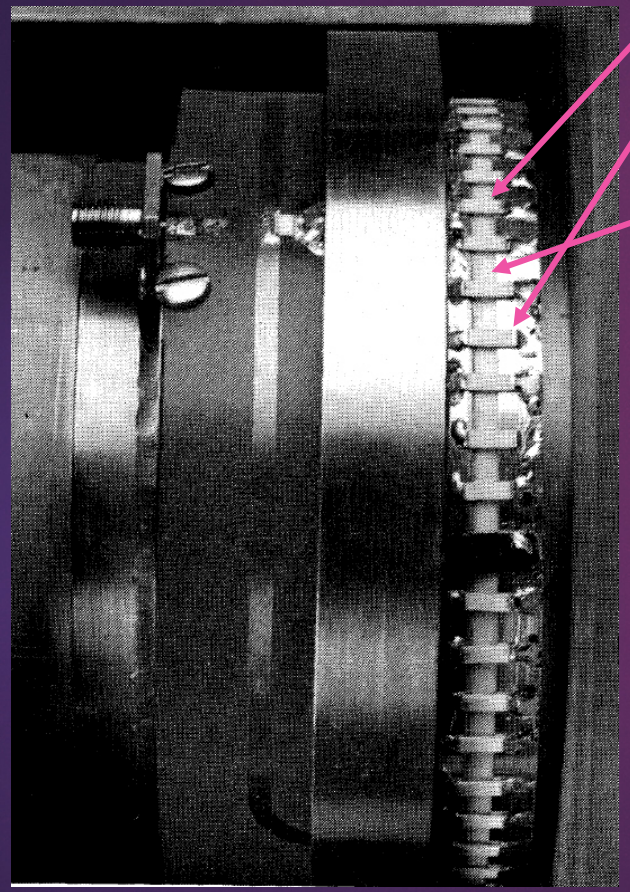

resistors

ceramic gap

peak current and longitudinal profiles of 6 bunches in RHIC

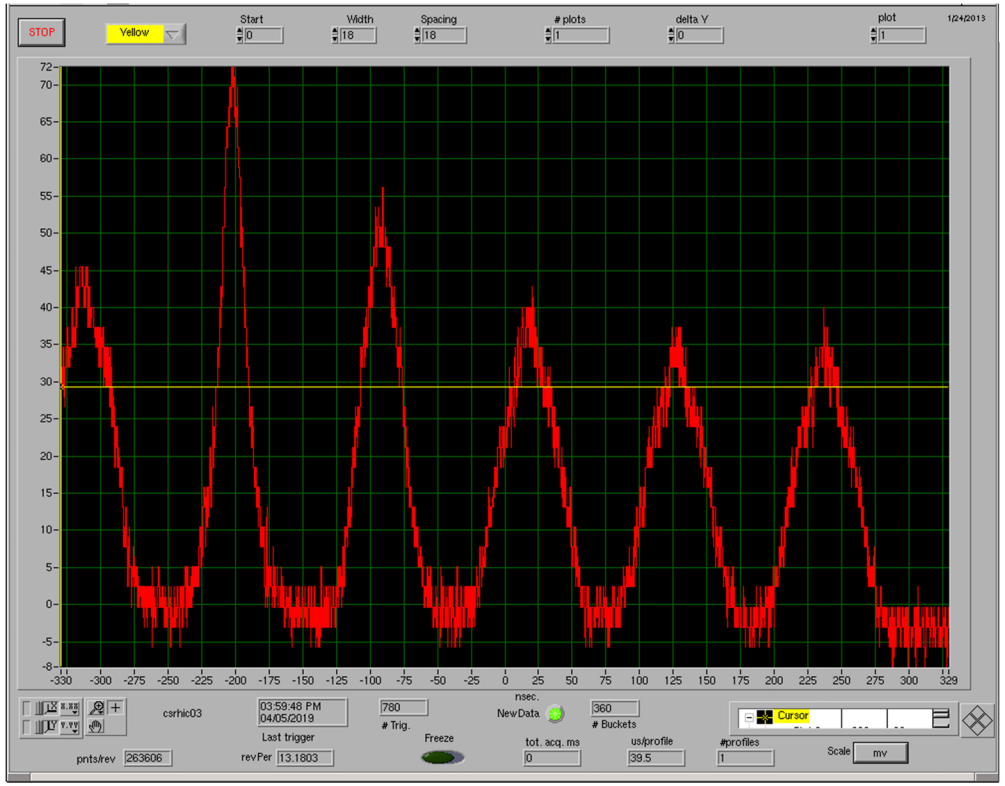

"Longitudinal Emittance: An Introduction to the Concept and Survey of Measurement Techniques Including Design of a Wall Current Monitor", R.C. Webber (FNAL, 1990)

"An Improved Resistive Wall Monitor", B. Fellenz and Jim Crisp, BIW (1998) for the FNAL main injector

Transverse Beam Position Measurements – Button BPMs

Buttons are a variant of the capacitive monitor (backup slides), but terminated into a characteristic impedance (usually by a coax cable with impedance 50 Ω). The response obtained must take into account the signal propagation (like for transmission line detectors, next section)

button electrodes

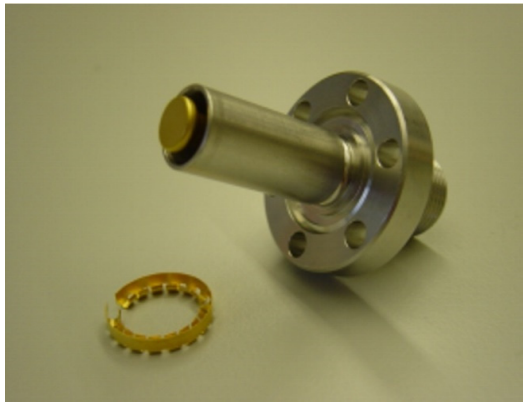

LHC 24 mm button with curved surface

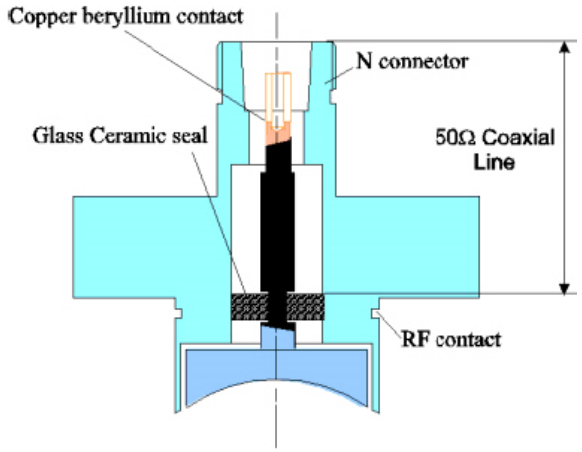

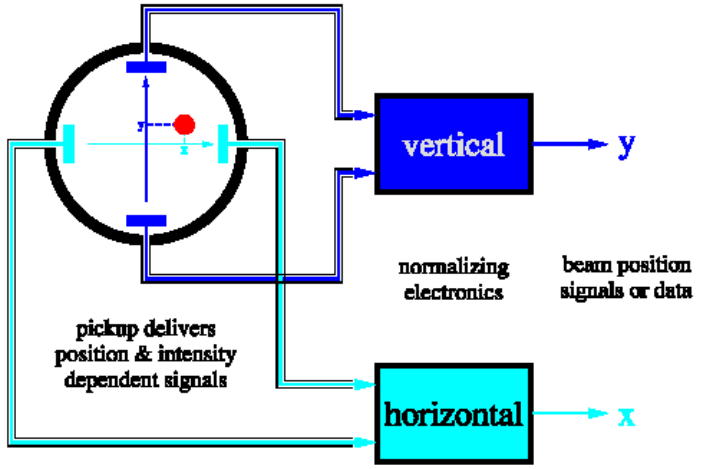

beam "position"

V_R-V_L (horizontal)

V_U-V_D (vertical)

beam intensity, e.g. V_R+V_L, V_U+V_D

normalized (intensity-independent) beam position given by ratio

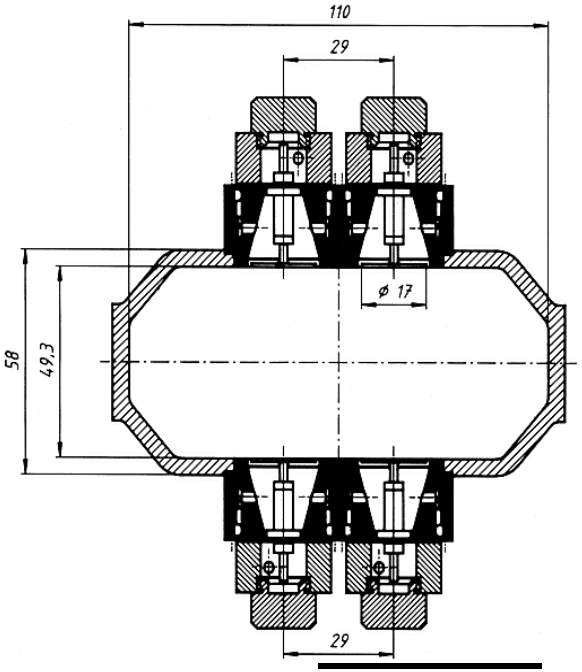

cross-sectional view of the button BPM assembly typical of synchrotron light facilities (here DORIS)

Challenges: dynamic range, impedances

Transverse Beam Position Measurements – Stripline BPMs

principle: electrode (spanning some azimuth) acts as an inner conductor of a coaxial line; shield acts as the grounded outer conductor

unterminated transmission line

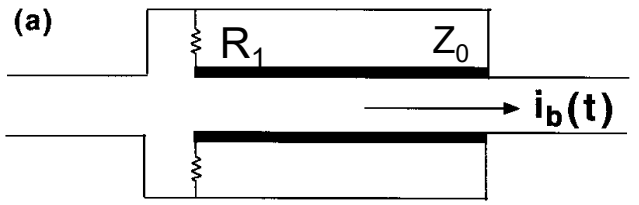

transmission line terminated (rhs) to a matched impedance

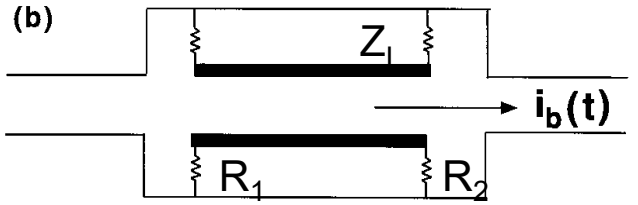

Signal propagation and development calculated using transmission line analysis with characteristic impedance Z_0 and terminated in a resistor R (

$$\rho = \text{reflection coefficient} = \frac{R-Z_0}{R+Z_0} = \begin{cases} 0 & \text{if } R=Z_0 \\ -1 & \text{if } R=0 \\ >0 & \text{if } R>Z_0 \\ <0 & \text{if } R<Z_0 \end{cases}$$

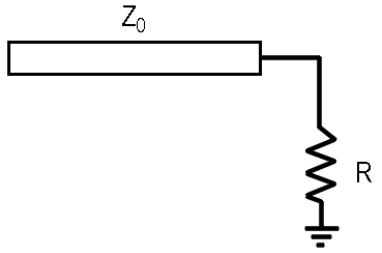

$\Gamma = (1-\rho)^{1/2}$ = transmission coefficient

With this, can show that case (b) above represents a ‘directional’ BPM (derivation given in backup slides)

Photo of a stripline BPM monitor

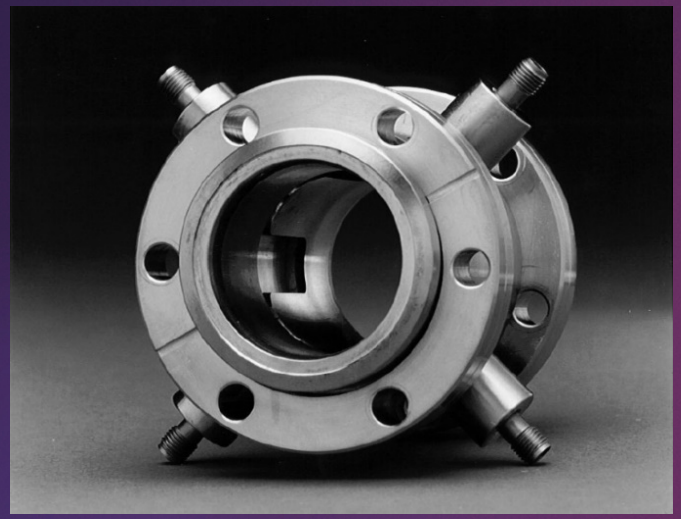

the LEUTL at Argonne shorted S-band quarter-wave four-plate stripline BPM (courtesy R.M. Lill)

sensitivity

$$|S| = |\frac{V}{i_w}| = R_1 |\sin^2 \omega \Delta t|$$

signal peaks at

$$\omega \Delta t = \frac{2\pi L}{\lambda} = \frac{\pi}{2} \longrightarrow L = \frac{\lambda}{4}$$

spacing between zeros

$$\omega \Delta t = 0 \longrightarrow L = \frac{\lambda}{2}$$

sensitivity of a matched transmission line detector of length L=10 cm

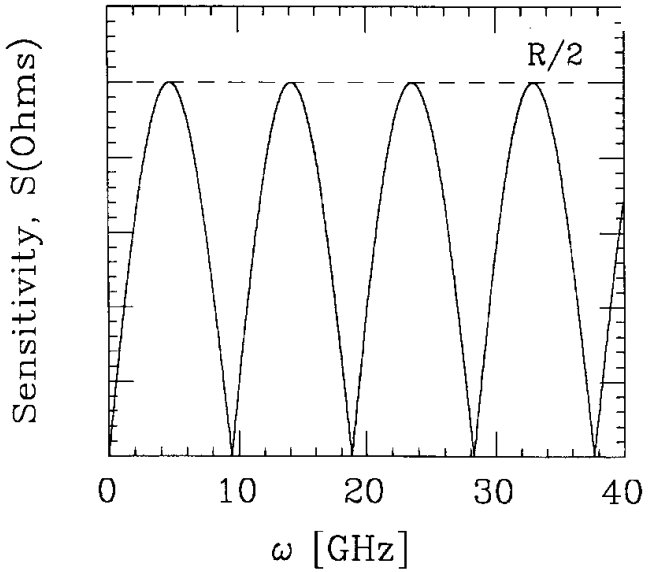

L=28 mm (electrical length ~7% longer than theoretical quarter-wavelength)

Transverse Beam Position Measurements – Cavity BPMs

principle: excitation of discrete modes (depending on bunch charge, position, and spectrum) in a resonant structure; detection of dipole mode signal proportional to bunch charge, q×transverse displacement, δx

provides high sensitivity (signal amplitude / displacement)

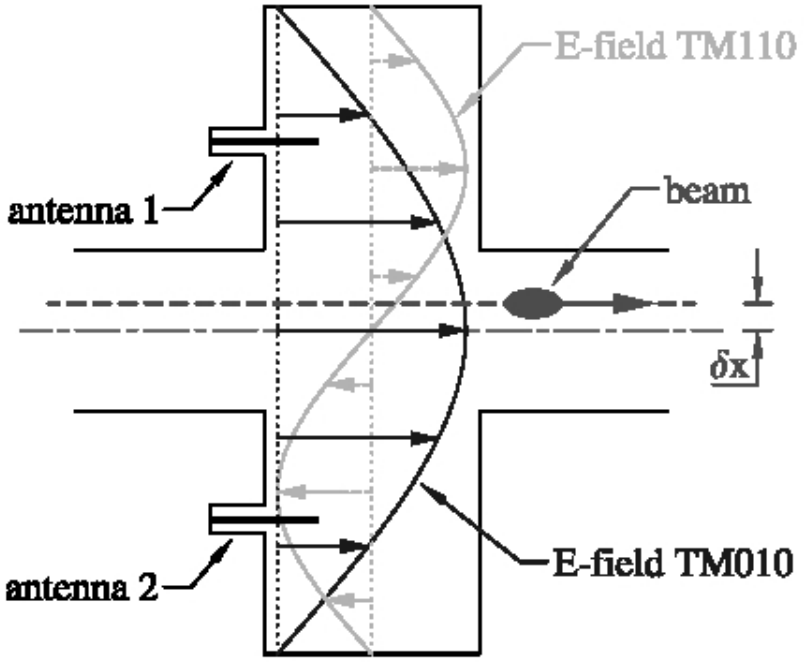

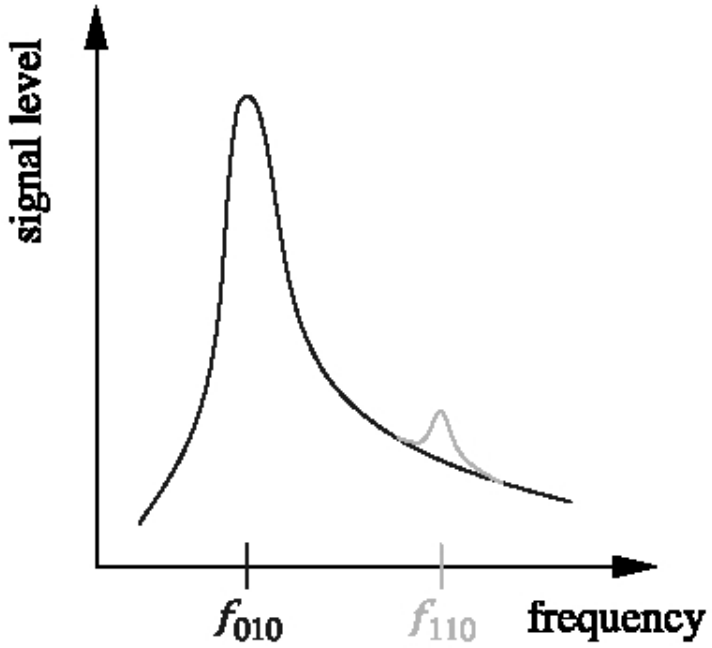

TM_{010}, "common mode" (∝ I)
TM_{110}, dipole mode of interest

} amplitude detected at position of antenna contains contributions from both modes → signal processing

"Cavity BPMs", R. Lorentz (BIW, Stanford, 1998)

pioneering experiments: 3 C-band cavity “RF” BPMs in series at the FFTB (SLAC)

→25 nm position resolution at 1 nC bunch charge

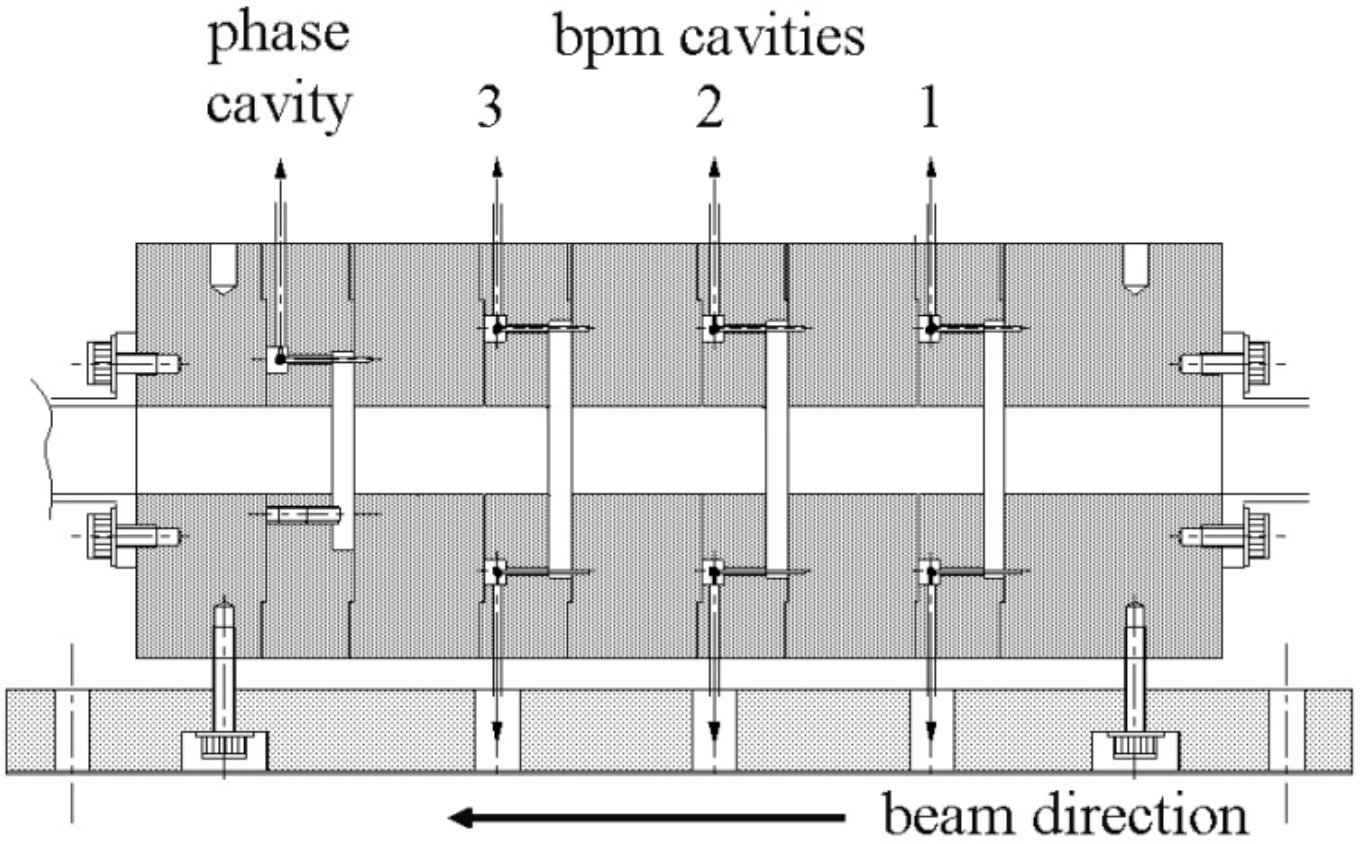

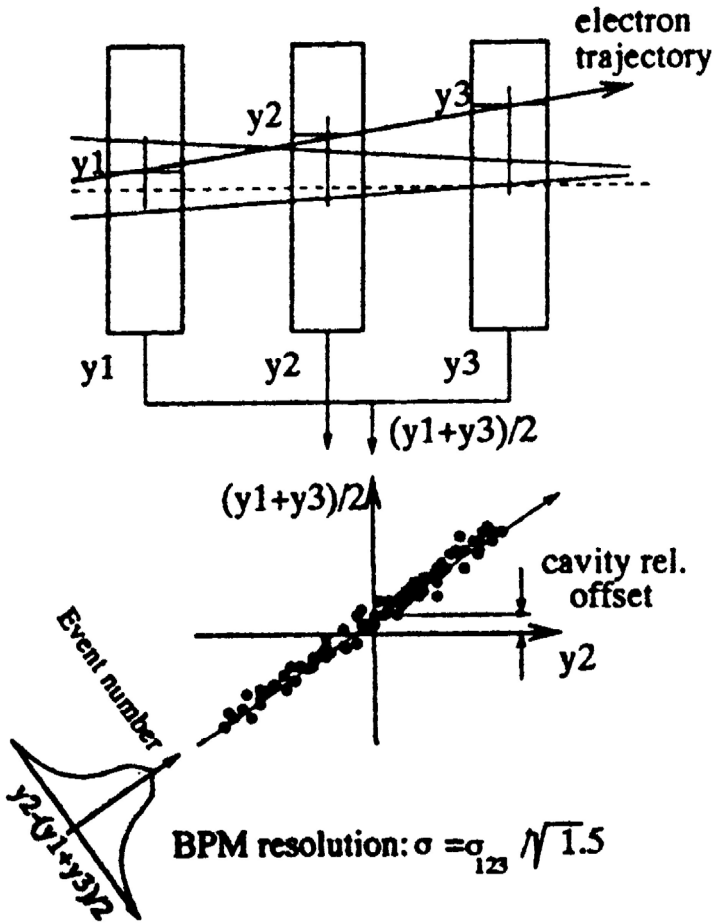

Challenges: impedances, fabrication tolerances

(courtesy, T. Shintake)

Transverse Beam Size Measurements - Screens

principle: intercepting screen (eg. Al_2O_3Cr possibly with phosphorescent coating) inserted into beam path (usually 45 deg); image viewed by camera → direct observation of x-y ($\eta = 0$) or y-δ ($\eta \neq 0$) distribution

fluorescence – light emitted (t~10 ns) as excited atoms decay to ground state
phosphorescence – light continues to emit (~ μs) after exciting mechanism has ceased (i.e. oscilloscope "afterglow")
luminescence – combination of both processes

R. Jung et al, "Single Pass Optical Profile Monitoring" (DIPAC 2003)

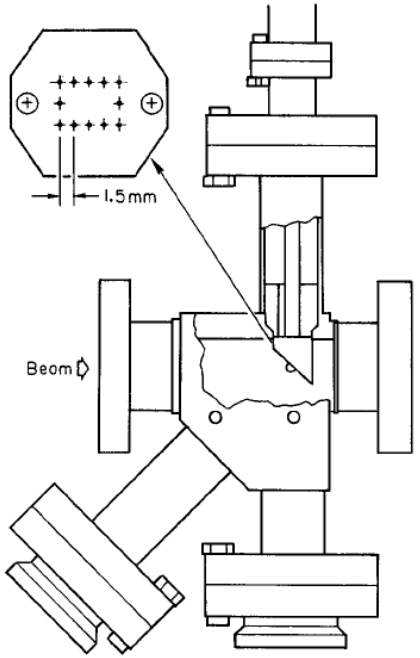

(courtesy P. Tenenbaum)

profile measurements
- image is digitized, projected, fitted with Gaussian
- calibration: often grid lines directly etched onto screen or with calibration holes drilled, either with known spacing

challenges
- spatial resolution (20-30 μm) given by phosphor grain size and phosphor transparency
- temporal resolution – given by decay time
- radiation hardness of screen and camera
- dynamic range (saturation of screen)

advantage
- x-y coupling immediately visible

Transverse Beam Size Measurements – Wire Scanners

principle: precision stage with precision encoder propels shaft with wire support wires (e.g. C, Be, or W) scanned across beam (or beam across wire), interaction of beam with wire detected

wire velocity: depends on desired interpoint spacing and on the bunch repetition frequency

methods of detection:

- change in voltage on wire induced by secondary emission
- hard Bremsstrahlung – forward directed γs which are separated from beam via an applied magnetic field and converted to e+/e- in the vacuum chamber wall and detected with a Cerenkov counter or PMT (after conversion to γs in front end of detector)
- via detection at 90 deg (δ-rays)
- using PMTs to detect scattering and electromagnetic showers
- (via change in tension of wire for beam-tail measurements)
- wire-beam interactions

CERN PS/PSB flying wire

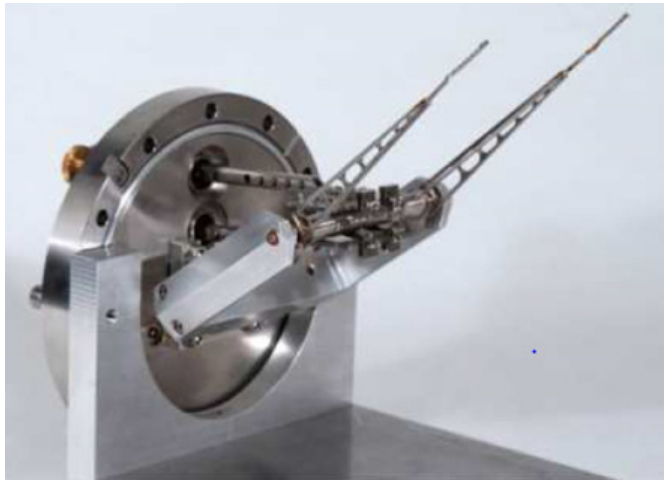

CERN SPS rotational wire

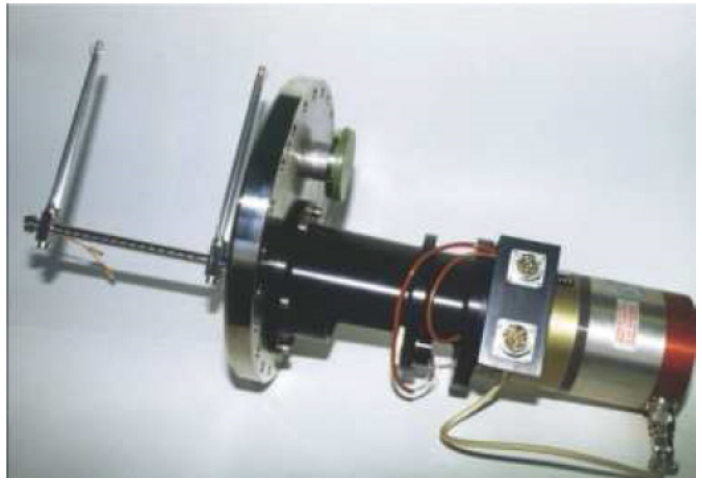

Photo of a wire scanner

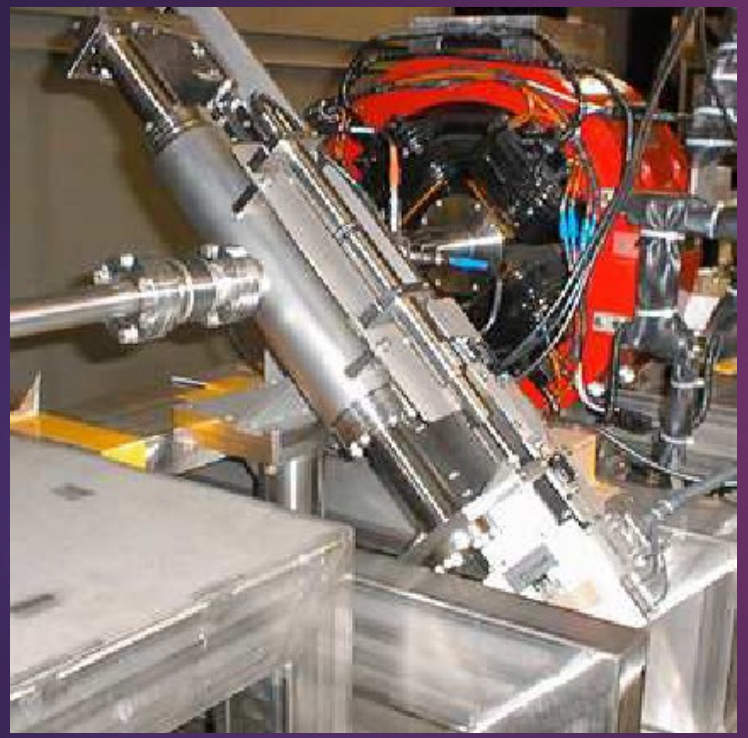

wire scanner chamber installed in the ATF (KEK) extraction line, courtesy H. Hayano

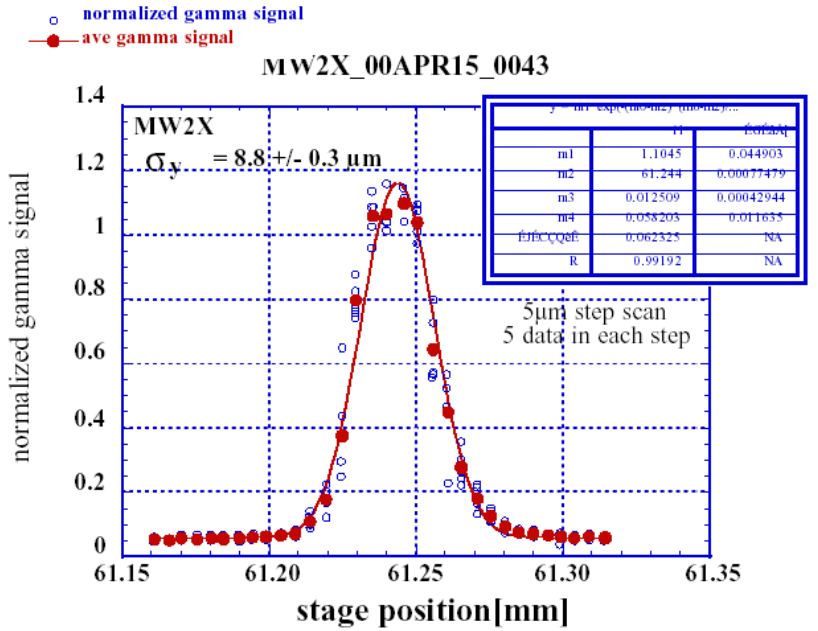

challenges

- different beam bunch for each data point
- no information on x-y coupling with 1 wire (need 3 wires at common location)
- dynamic range: saturation of detectors (PMTs)
- single-pulse beam heating
- wire thickness (adds in quadrature with beam size)
- higher-order modes
- impact on environment (downstream quench in SC accelerators)

Noninvasive transverse beam size measurements – ionization profile monitors

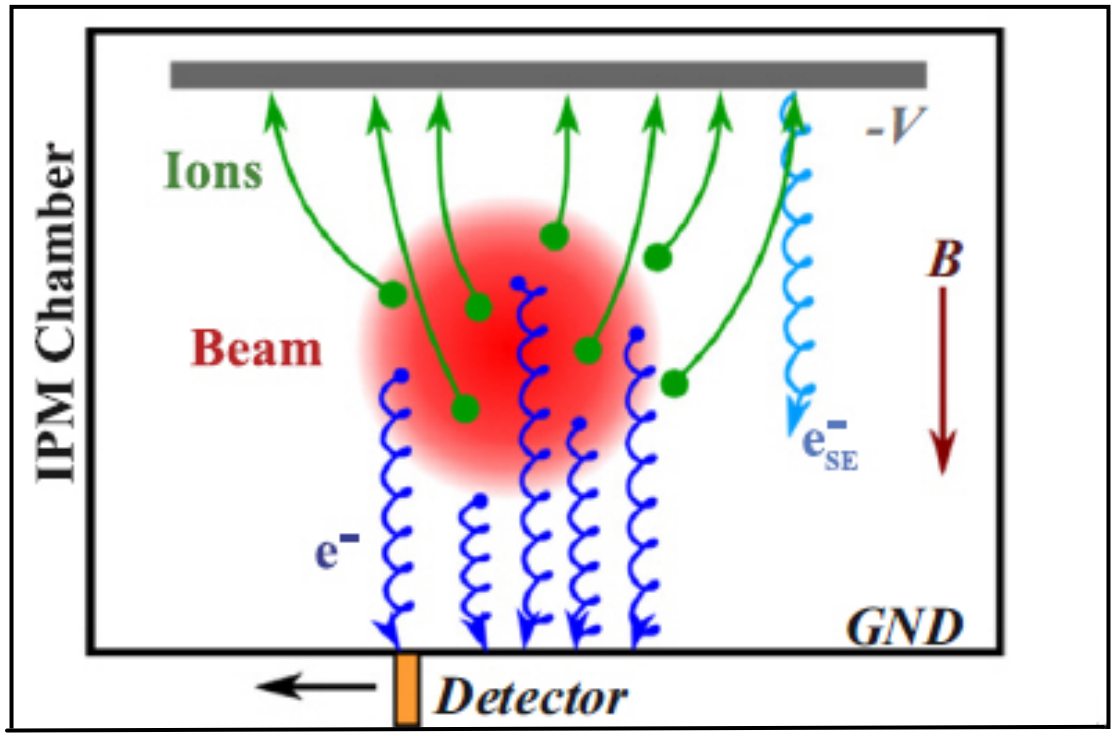

principle:

measure the distribution of ions and/or electrons created by ionization in the beam transport channel (either with intentional introduction of local pressure bump or from residual gas)

From D.A. Barkoski et al, Nucl. Instr. And Meth. A 767 (2014) 379-384.

photo of an IPM (at RHIC, BNL)

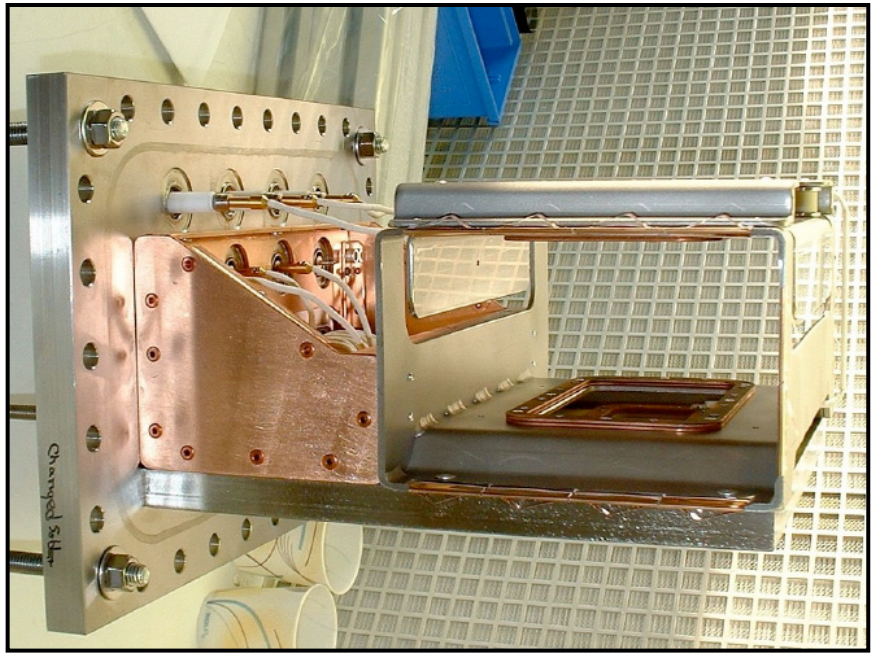

sample measurements

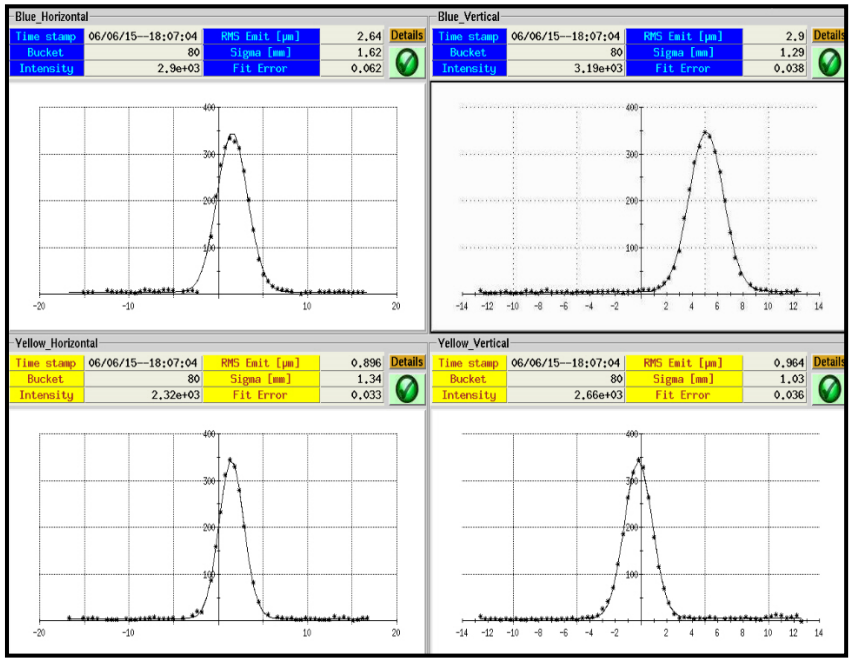

challenges (design evolution):

- sensitivity to beam loss
- electron clouds
- MCP depletion and dynamic MCP saturation
- rf coupling from beam

time-averaged profiles if event rate low

space charge

- of the liberated ions (if detecting ions)
- effect of primary beam on the liberated electrons

emittance evolution

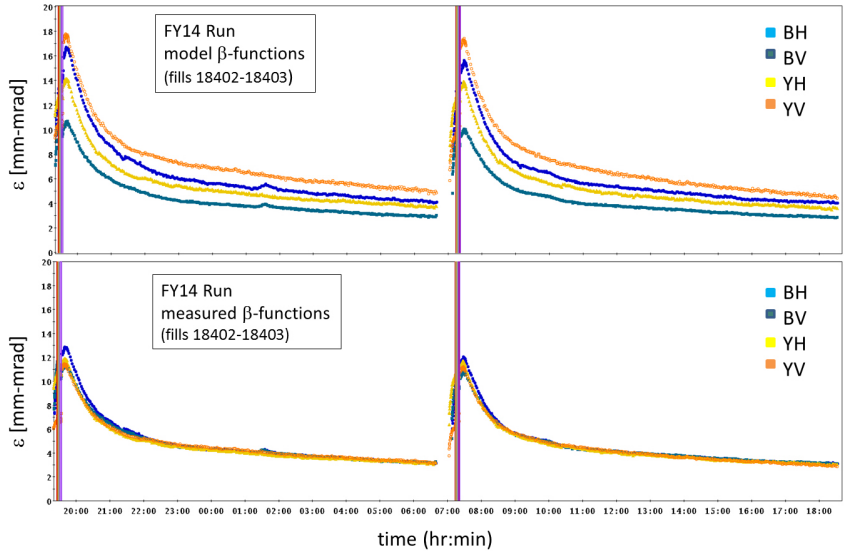

Noninvasive Transverse Beam Size Measurements – Fluorescence Monitors

principle

emission of optical photons due to de-excitation of ionized gas

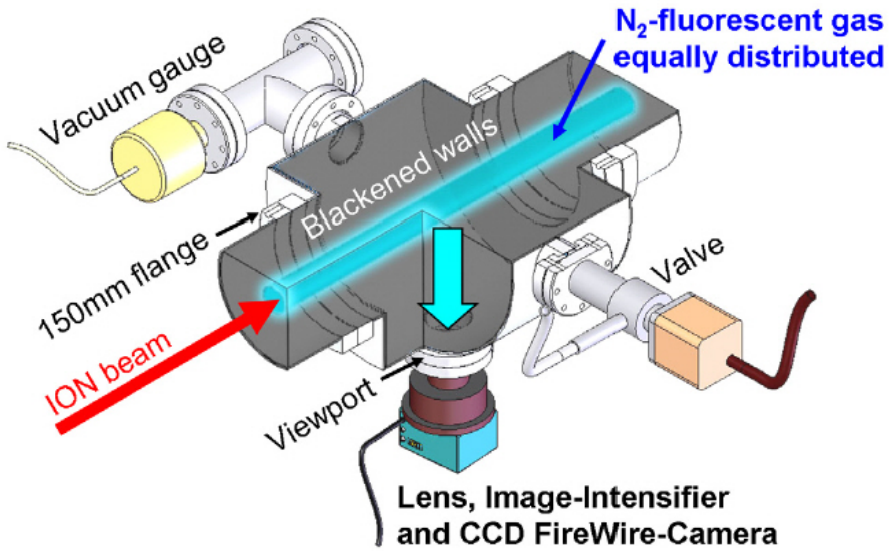

challenges

gas composition

temporal resolution – given by decay time

space charge?

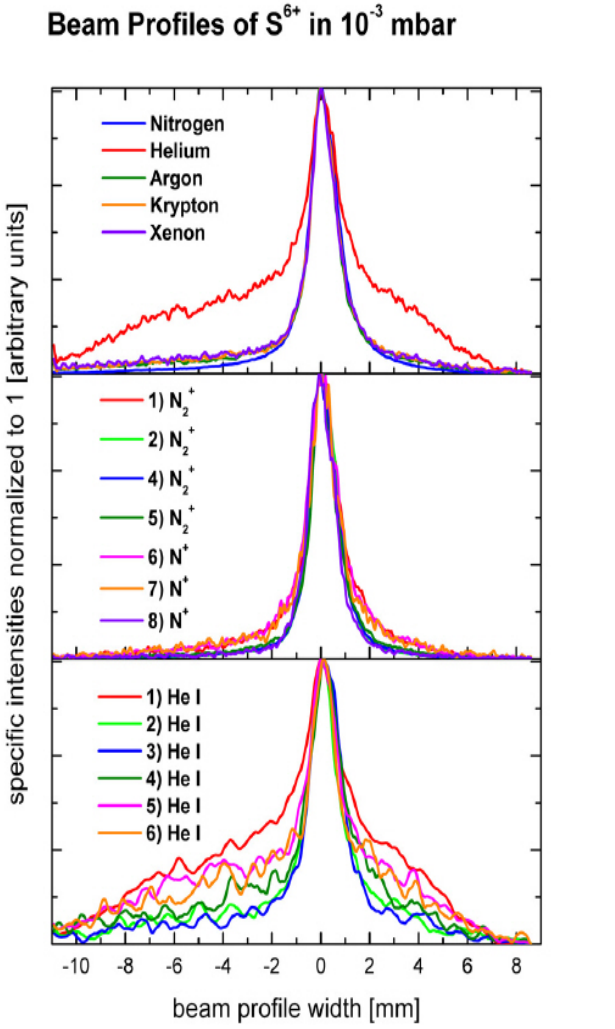

Figure 5: Gas specific beam profiles (upper plot) and transition specific beam profiles of nitrogen (middle) and helium

P. Forck et al, Beam induced fluorescence profile monitor developments, HB2010

Noninvasive Transverse Beam Profiles – Laser Profile Monitors

principle: laser used to neutralize H^- (1 proton, 2 electrons) beam producing H^0 and a liberated electron

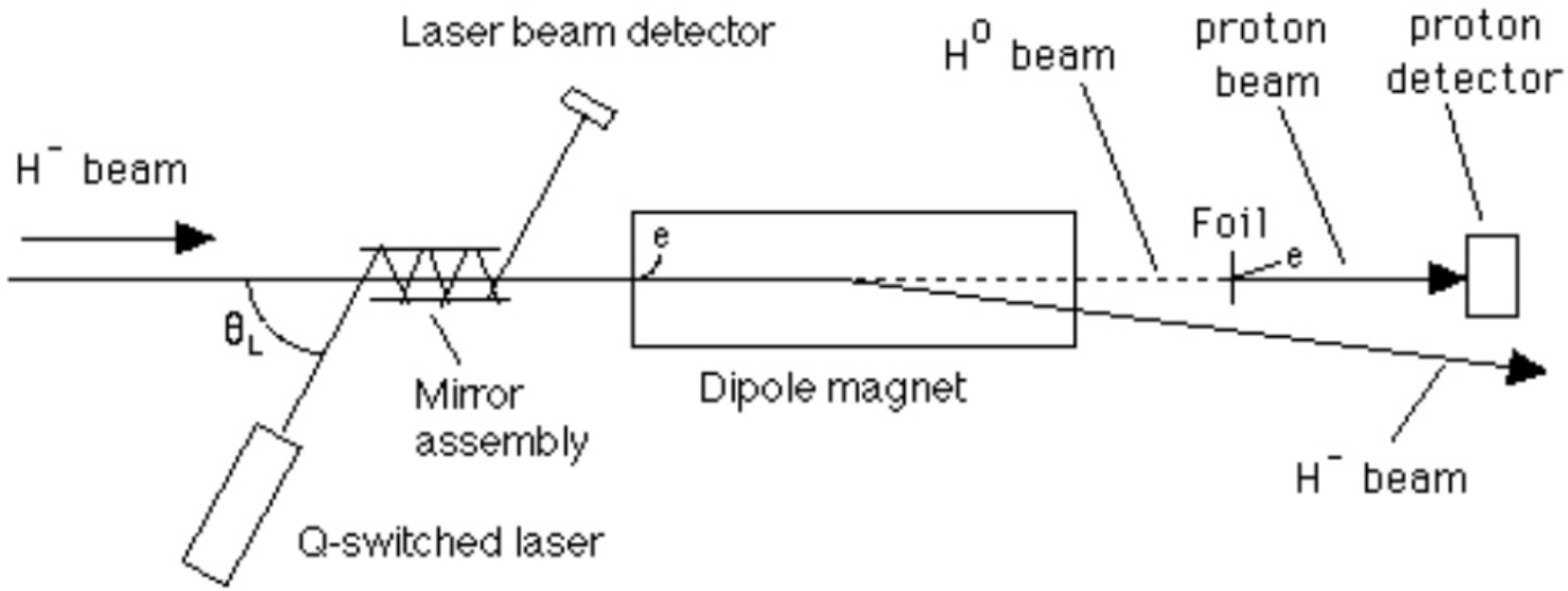

many geometries and detector options
here: forward propagating H^0
current modulation of H-
electron detection

Figure from Laser Diagnostics for High Current Beams, R.E. Schafer, BIW (1998)

Laser Profile Monitor at the SNS Superconducting Linac

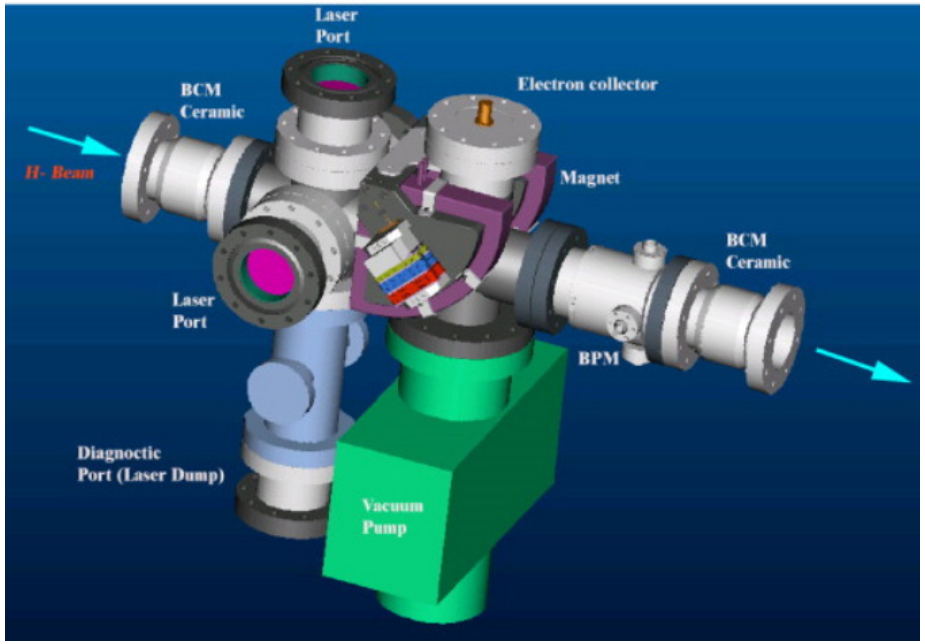

challenges

- laser alignment and focus spot size
- optical aberrations
- mechanical vibrations
- temperature stability of laser transport line

additional advantage – no debris (e.g. broken wires) in superconducting cavities

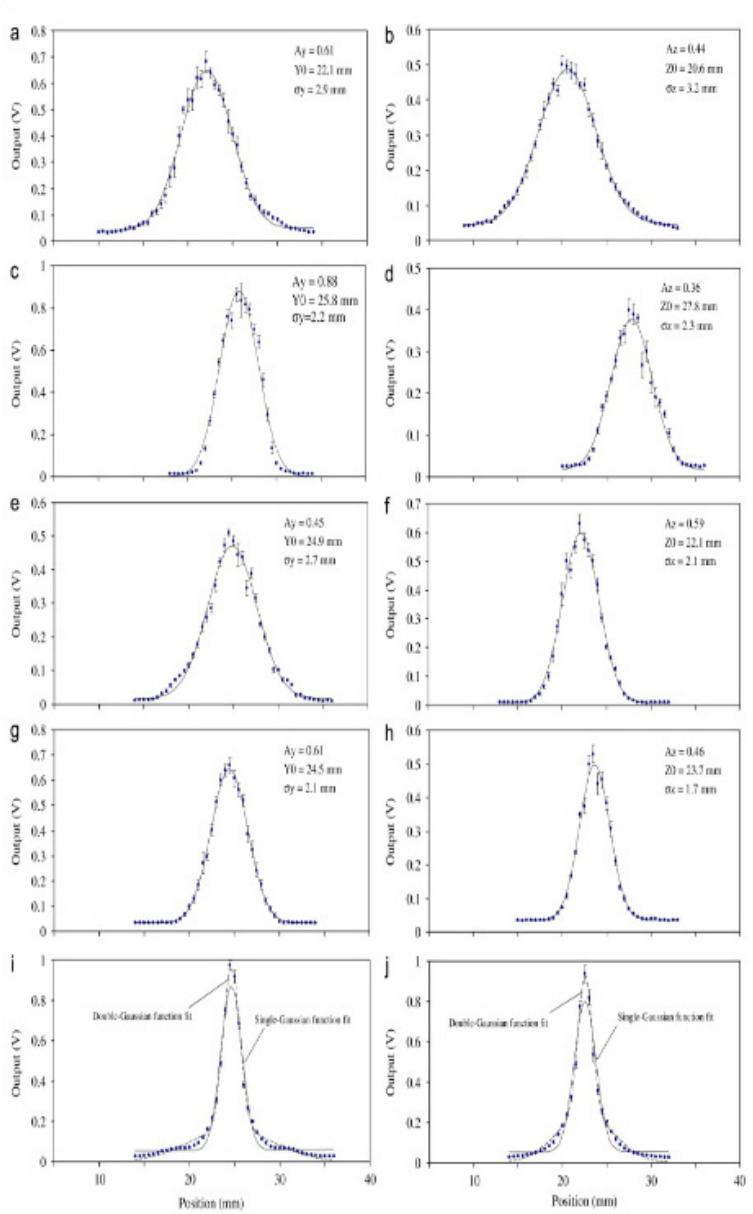

Laser wire beam profile monitor in the spallation neutron source (SNS) superconducting linac, Y. Liu et al, Nucl. Instr. And Meth. 612 (2010) 241-253

Noninvasive Transverse Beam Profiles – Laser Wire Scanners

principle: laser wire provides a non-invasive and non-destructable target wire scanned across beam (or beam across wire)

detect forward scattered Compton γs or lower-energy electrons after deflection by a magnetic field

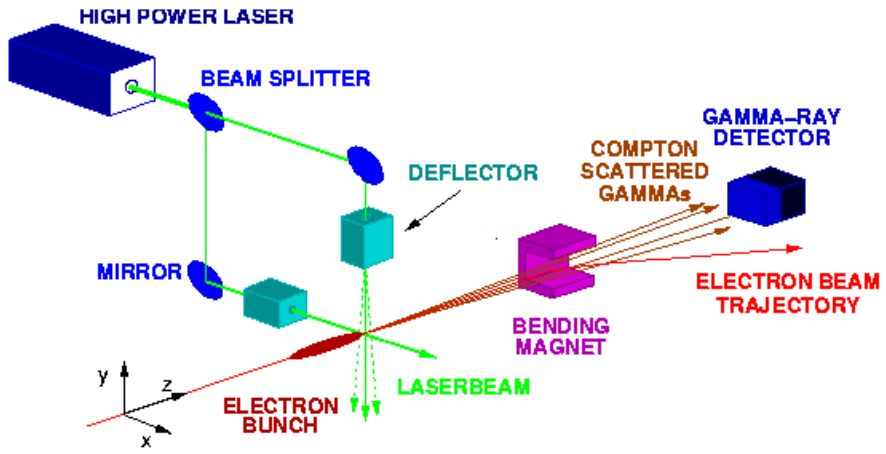

schematic of the laser wire system at the third generation synchrotron light source PETRA 3 (courtesy S. Schreiber)

high power pulsed laser

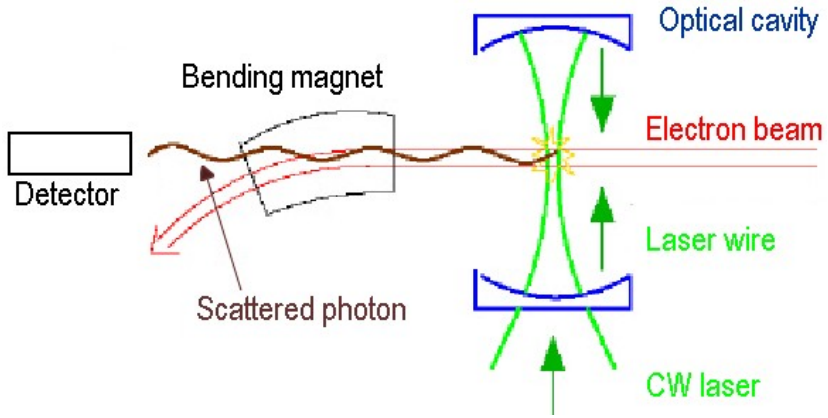

overview of the laser wire system at the KEK ATF (courtesy H. Sakai)

optical cavity pumped by CW laser (mirror reflectivity ~99+%)

laser wire measurement at the KEK ATF

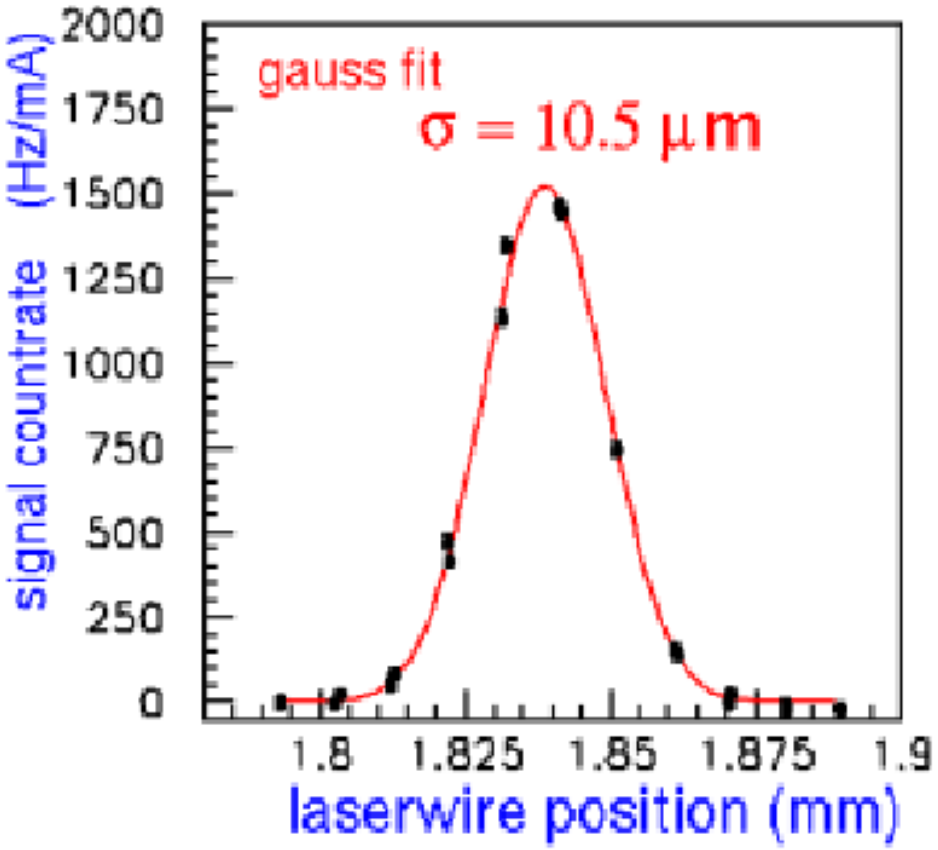

$$\sigma_y = \sqrt{{\sigma_{obs}}^2 - (\frac{w_0}{2})^2}$$

$$\beta_y \epsilon_y = (\sigma_y)^2 - (\eta_y \frac{\sigma_p}{p})^2$$

as with normal wires, the wire size must be taken into account

(here w_0 is the 2σ wire thickness)

challenges

- waist of laser < beam size (in practice, waist size ~λ)
- background and background subtraction
- depth of focus
- synchronization (for pulsed lasers)

(courtesy H. Sakai)

Bunch Length – Transverse Mode Cavities (1965: Miller,Tang, Koontz)

principle

- use transverse mode deflecting cavity to kick kicks the beam, introducing and x-z correlation
- Bunch detected using profile monitor
  - directly downstream at high-η location
  - off-axis using additional phase offset (static centroid kick)

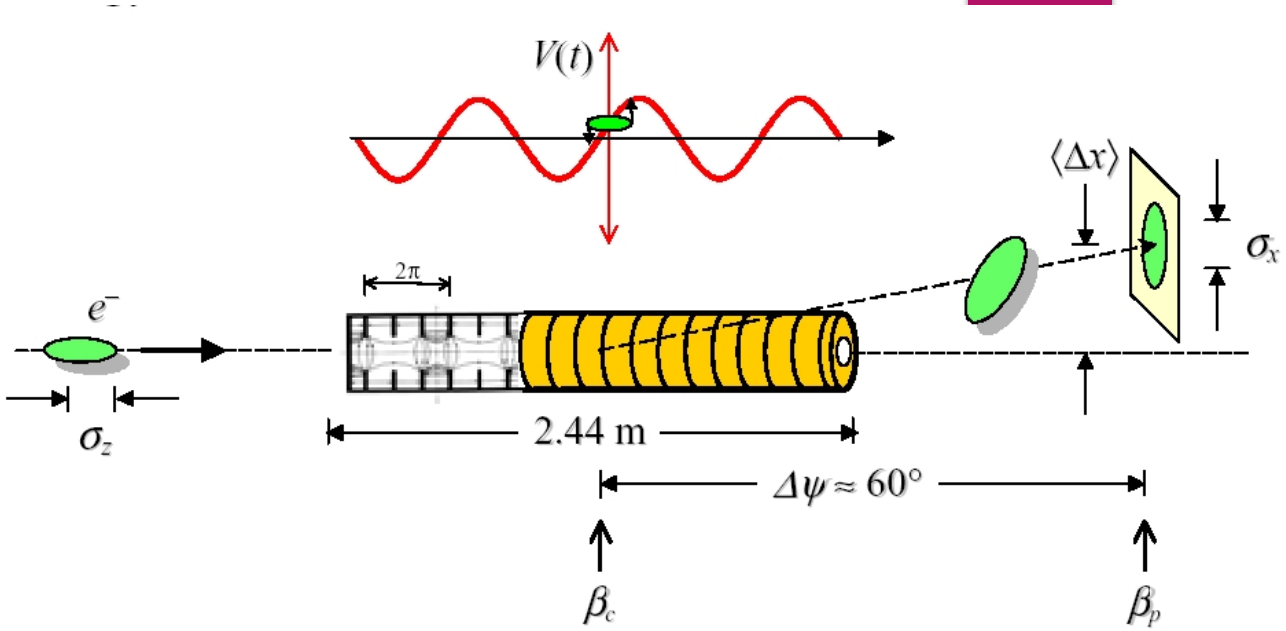

screen image and slice projection (LEReC)

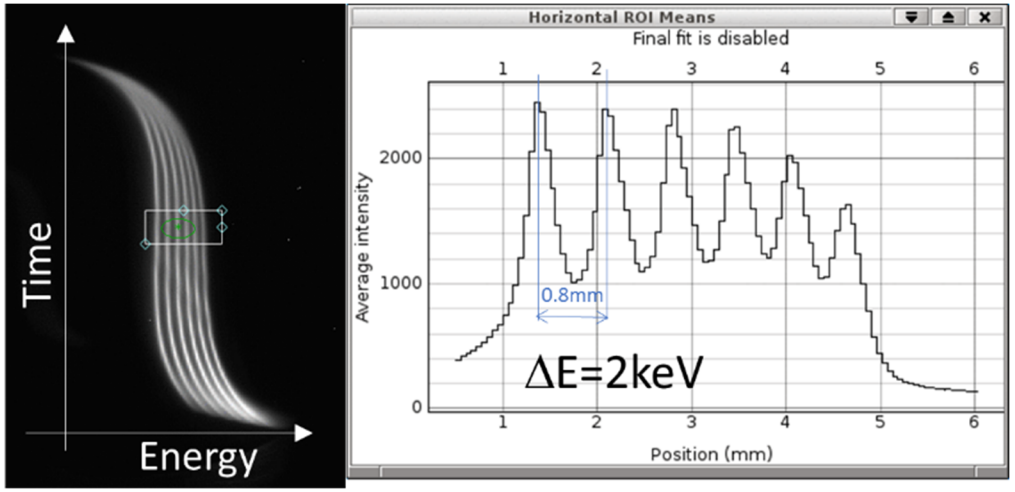

bunch length scan (test for LCLS)

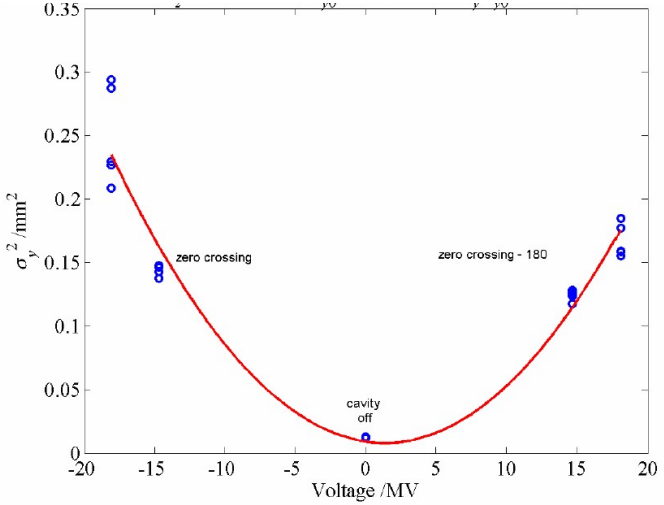

$\sigma_y^2 = A(V_{rf}-V_{rf,min})^2 = \sigma_{y0}^2$

$\sigma_z = A^{1/2}E_0\lambda_{rf}/2\pi R_{34}$

A is a fitted parameter, A

(courtesy R. Akre)

Measuring beam parameters and characterizing accelerator performance

- transverse emittances ε
- betatron tunes Q
- beta functions β
- coupling κ
- chromaticity ξ, Q'

Emittance Measurements

Beam transport $\begin{pmatrix} x \\ x' \end{pmatrix}_f = \begin{pmatrix} R_{11} & R_{12} \\ R_{21} & R_{22} \end{pmatrix}_{fi} \begin{pmatrix} x \\ x' \end{pmatrix}_i$

transformation of the phase space coordinates (x,x') of a single particle (from i→f) given in terms of the transport matrix, R

Equivalently, and complementarily, the Twiss parameters (α, β, and γ) obey

$$\begin{pmatrix} \beta \\ \alpha \\ \gamma \end{pmatrix}_f = \begin{pmatrix} R_{11}^2 & -2R_{11}R_{12} & R_{12}^2 \\ -R_{11}R_{21} & 1+2R_{12}R_{21} & -R_{12}R_{22} \\ R_{21}^2 & -2R_{21}R_{22} & R_{22}^2 \end{pmatrix}_{fi} \begin{pmatrix} \beta \\ \alpha \\ \gamma \end{pmatrix}_i$$

The elements of the transfer matrix R are given generally by

$$\mathbf{R}_{fi} = \begin{pmatrix} \sqrt{\frac{\beta_f}{\beta_i}}(\cos\phi_{fi} + \alpha_i \ \sin\phi_{fi}) & \sqrt{\beta_f\beta_i} \ \sin\phi_{fi} \\ -\frac{1+\alpha_f\alpha_i}{\sqrt{\beta_f\beta_i}} \ \sin\phi_{fi} + \frac{\alpha_i-\alpha_f}{\sqrt{\beta_f\beta_i}} \ \cos\phi_{fi} & \sqrt{\frac{\beta_i}{\beta_f}} \ (\cos\phi_{fi} - \alpha_f \ \sin\phi_{fi}) \end{pmatrix}$$

or if the initial and final observations points are the same, by the one-turn-map:

$$\mathbf{R}_{\mathrm{otm}} = \begin{pmatrix} \cos\mu + \alpha \ \sin\mu & \beta \ \sin\mu \\ -\gamma\sin\mu & \cos\mu - \alpha \ \sin\mu \end{pmatrix}$$

where μ is the 1-turn phase advance: $\mu = 2\pi Q$

A third equivalent approach involves the beam matrix defined as

$$\Sigma^x_{\text{beam}} = \epsilon_x \begin{pmatrix} \beta & -\alpha \\ -\alpha & \gamma \end{pmatrix}$$

in terms of Twiss parameters

$$= \begin{pmatrix} \langle x^2 \rangle - \langle x \rangle^2 & \langle xx' \rangle - \langle x \rangle \langle x' \rangle \\ \langle x'x \rangle - \langle x' \rangle \langle x \rangle & \langle x'^2 \rangle - \langle x' \rangle^2 \end{pmatrix}$$

in terms of the moments of the beam distribution

Here <x> and <x^2> are the first and second moments of the beam distribution:

$$\langle x \rangle = \frac{\int_0^\infty x f(x)\,\mathrm{d}x}{\int_0^\infty f(x)\,\mathrm{d}x} \qquad \langle x^2 \rangle = \frac{\int_0^\infty x^2 f(x)\,\mathrm{d}x}{\int_0^\infty f(x)\,\mathrm{d}x}$$

where f(x) is the beam intensity distribution

The transformation of the initial beam matrix $\Sigma_{\text{beam},0}$ to the desired observation point is

$$\Sigma_{\text{beam}} = R \Sigma_{\text{beam},0} R^t$$

where R is again the transfer matrix

Neglecting the mean of the distribution (disregarding the static position offset of the core of the beam; i.e. <x>=0) :

$$\Sigma^x_{\text{beam}} = \begin{pmatrix} \langle x^2 \rangle & \langle xx' \rangle \\ \langle xx' \rangle & \langle x'^2 \rangle \end{pmatrix}$$

and the root-mean-square (rms) of the distribution is

$$\sigma_x = \langle x^2 \rangle^{\frac{1}{2}}$$

Method I: quadrupole scan

principle: with a well-centered beam, measure the beam size as a function of the quadrupole field strength

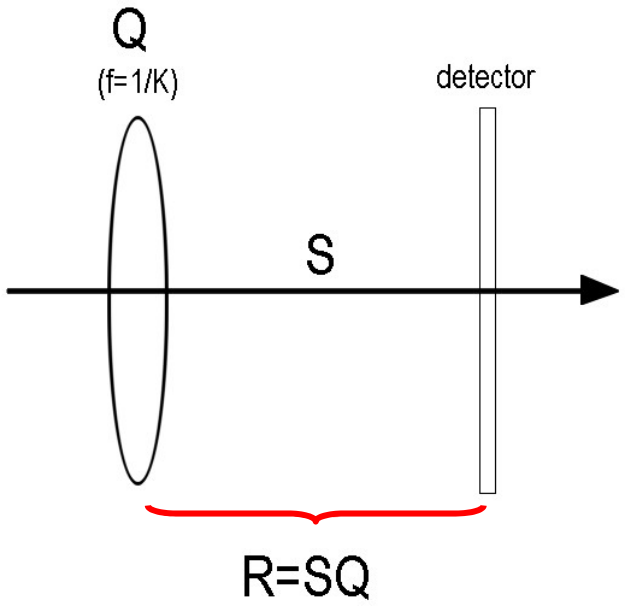

Here
Q is the transfer matrix of the quadrupole
R is the transfer matrix between the quadrupole and the beam size detector

With $Q = \begin{pmatrix} 1 & 0 \\ K & 1 \end{pmatrix}$ then $R = \begin{pmatrix} S_{11} + KS_{12} & S_{12} \\ S_{21} + KS_{22} & S_{22} \end{pmatrix}$ with $\Sigma_{\text{beam}} = R\Sigma_{\text{beam},0}R^t$

The (11)-element of the beam transfer matrix is found after algebra to be:

$$\Sigma_{11}(= \langle x^2 \rangle) = ({S_{11}}^2\Sigma_{11_0} + 2S_{11}S_{12}\Sigma_{12_0} + {S_{12}}^2\Sigma_{22_0}) + (2S_{11}S_{12}\Sigma_{11_0} + 2{S_{12}}^2\Sigma_{12_0})K_o + {S_{12}}^2\Sigma_{11}K^2$$

which is quadratic in the field strength, K

Measurement: measure beam size versus quadrupole field strength

recall: $$\Sigma_{11}(=\langle x^2\rangle) = ({S_{11}}^2\Sigma_{11_o} + 2S_{11}S_{12}\Sigma_{12_o} + {S_{12}}^2\Sigma_{22_o}) + (2S_{11}S_{12}\Sigma_{11_o} + 2{S_{12}}^2\Sigma_{12_o})K + {S_{12}}^2\Sigma_{11}K^2$$

data:

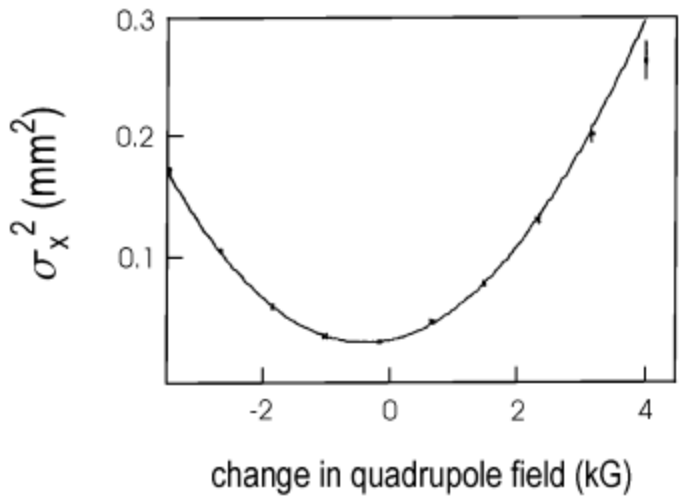

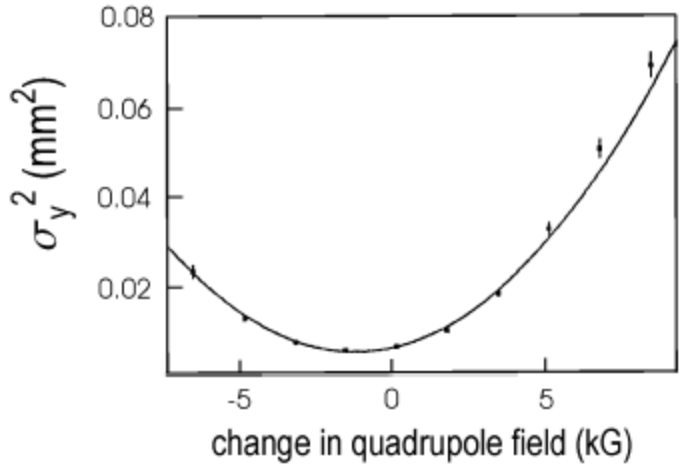

fitting function (parabolic):

$$\Sigma_{11} = A(K-B)^2 + C = AK^2 - 2ABK + (C + AB^2)$$

equating terms (drop subscripts ‘o’),

$$A = S_{12}^2\Sigma_{11}\,,$$

$$-2AB = 2S_{11}S_{12}\Sigma_{11} + 2S_{12}^2\Sigma_{12}\,,$$

$$C + AB^2 = {S_{11}}^2\Sigma_{11} + 2S_{11}S_{12}\Sigma_{12} + {S_{12}}^2\Sigma_{22}$$

solving for the beam matrix elements:

$$\Sigma_{11} = A/{S_{12}}^2\,,$$

$$\Sigma_{12} = -\frac{A}{{S_{12}}^2}\left(B + \frac{S_{11}}{S_{12}}\right)\,,$$

$$\Sigma_{22} = \frac{1}{{S_{12}}^2}\left[(AB^2 + C) + 2AB\left(\frac{S_{11}}{S_{12}}\right) + A\left(\frac{S_{11}}{S_{12}}\right)^2\right]$$

The emittance is given from the determinant of the beam matrix:

$$\epsilon_x = \sqrt{\det\ \Sigma^x_{\rm beam}}$$

$$\begin{aligned}\det\ \Sigma^x_{\rm beam} &= \Sigma_{11}\Sigma_{22} - {\Sigma_{12}}^2 \\ &= AC/S_{12}^4\,,\end{aligned}$$

$$\Rightarrow\quad \epsilon_x = \sqrt{AC}/S_{12}^2$$

With these 3 fit parameters (A,B, and C), the 3 Twiss parameters are also known:

$$\beta_x = \frac{\Sigma_{11}}{\epsilon} = \sqrt{\frac{A}{C}}\,,$$

$$\alpha_x = -\frac{\Sigma_{12}}{\epsilon} = \sqrt{\frac{A}{C}}\left(B + \frac{S_{11}}{S_{12}}\right)\,,$$

$$\gamma_x = \frac{{S_{12}}^2}{\sqrt{AC}}\left[(AB^2 + C) + 2AB\left(\frac{S_{11}}{S_{12}}\right) + A\left(\frac{S_{11}}{S_{12}}\right)^2\right]$$

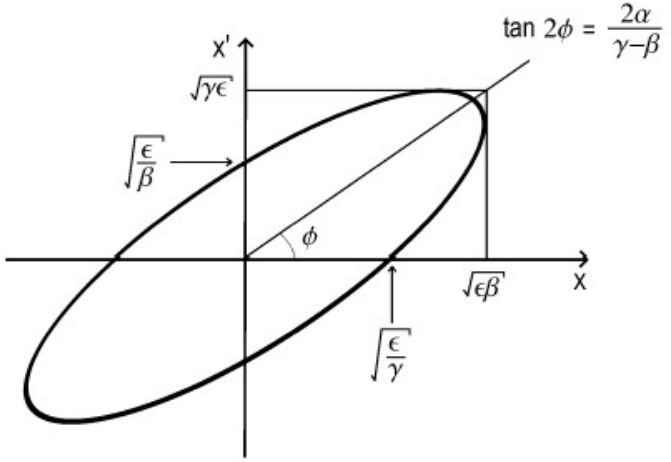

as a useful check, the beam-ellipse parameters should satisfy $(\beta_x\gamma_x\text{-}1)=\alpha^2$

Method II: fixed optics, measure beam size using multiple measurement devices

Recall: the matrix used to transport the Twiss parameters:

$$\begin{pmatrix}\beta\\ \alpha\\ \gamma\end{pmatrix}_f = \begin{pmatrix} R_{11}^2 & -2R_{11}R_{12} & R_{12}^2 \\ -R_{11}R_{21} & 1+2R_{12}R_{21} & -R_{12}R_{22} \\ R_{21}^2 & -2R_{21}R_{22} & R_{22}^2 \end{pmatrix}_{fi} \begin{pmatrix}\beta\\ \alpha\\ \gamma\end{pmatrix}_i$$

with fixed optics and multiple measurements of σ at different locations:

$$\underbrace{\begin{pmatrix} (\sigma_x^{(1)})^2 \\ (\sigma_x^{(2)})^2 \\ (\sigma_x^{(3)})^2 \\ \cdots \\ (\sigma_x^{n})^2 \end{pmatrix}}_{\Sigma_x} = \underbrace{\begin{pmatrix} (R_{11}^{(1)})^2 & 2R_{11}^{(1)}R_{12}^{(1)} & (R_{12}^{(1)})^2 \\ (R_{11}^{(2)})^2 & 2R_{11}^{(2)}R_{12}^{(2)} & (R_{12}^{(2)})^2 \\ (R_{11}^{(3)})^2 & 2R_{11}^{(3)}R_{12}^{(3)} & (R_{12}^{(3)})^2 \\ \cdots & & \\ (R_{11}^{(n)})^2 & R_{11}^{(n)}R_{12}^{(n)} & (R_{12}^{(n)})^2 \end{pmatrix}}_{B} \underbrace{\begin{pmatrix} \beta(s_0)\epsilon \\ -\alpha(s_0)\epsilon \\ \gamma(s_0)\epsilon \end{pmatrix}}_{o}$$

simplify notation:

$$\Sigma_x = \mathbf{B}\cdot\mathbf{o}$$

goal is to determine the vector o by minimizing the sum (least squares fit):

$$\chi^2 = \sum_{l=1}^{n} \frac{1}{\sigma^2_{\Sigma_x^{(l)}}} \left(\Sigma_x^{(l)} - \sum_{i=1}^{3} B_{li}o_i\right)^2$$

with the symmetric n×n covariance matrix, $\mathbf{T} = (\hat{\mathbf{B}}^t \cdot \hat{\mathbf{B}})^{-1}$

➡ the least-squares solution is $\mathbf{o} = \mathbf{T}\cdot\hat{\mathbf{B}}^t\cdot\hat{\Sigma}_x$

(the 'hats' show weighting: $\hat{B}_{li} = \frac{B_{li}}{\sigma_{\Sigma_x^{(l)}}}$ $\hat{\Sigma}_x^{(l)} = \frac{\Sigma_x^{(l)}}{\sigma_{\Sigma_x^{(l)}}}$)

once the components of o are known,

$$\epsilon = \sqrt{o_1 o_3 - o_2^2},$$
$$\beta = o_1/\epsilon, \text{ and}$$
$$\alpha = -o_2/\epsilon.$$

graphical representation of results:

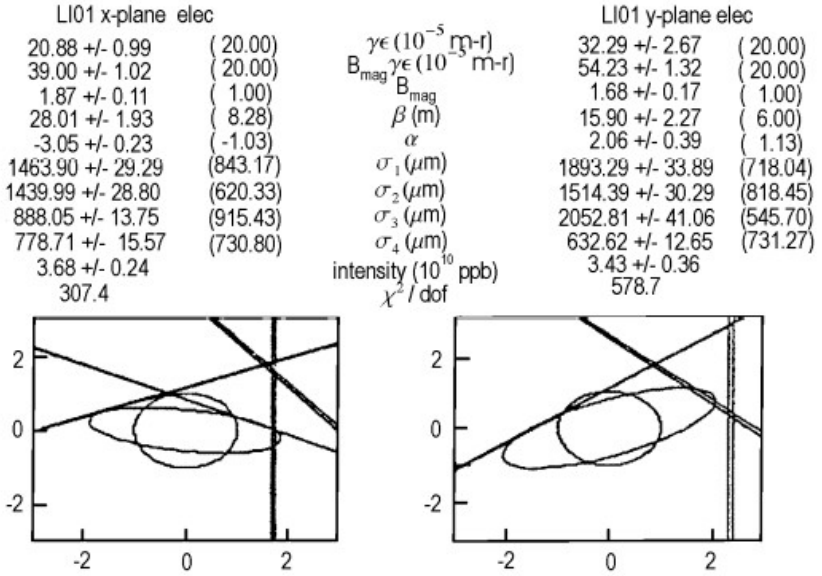

note: coordinate axes are so normalized (design phase ellipse is a circle):

$$\left(\frac{x}{\sqrt{\beta_x}}, \frac{\alpha_x x + \beta_x x'}{\sqrt{\beta_x}}\right)$$

lines show phase space coverage of wires:

$$\begin{pmatrix} x \\ x' \end{pmatrix}_{\text{ref point}} = R^{-1} \begin{pmatrix} \sigma_{x,w} \\ x'_w \end{pmatrix}$$

data: from the SLC injector linac

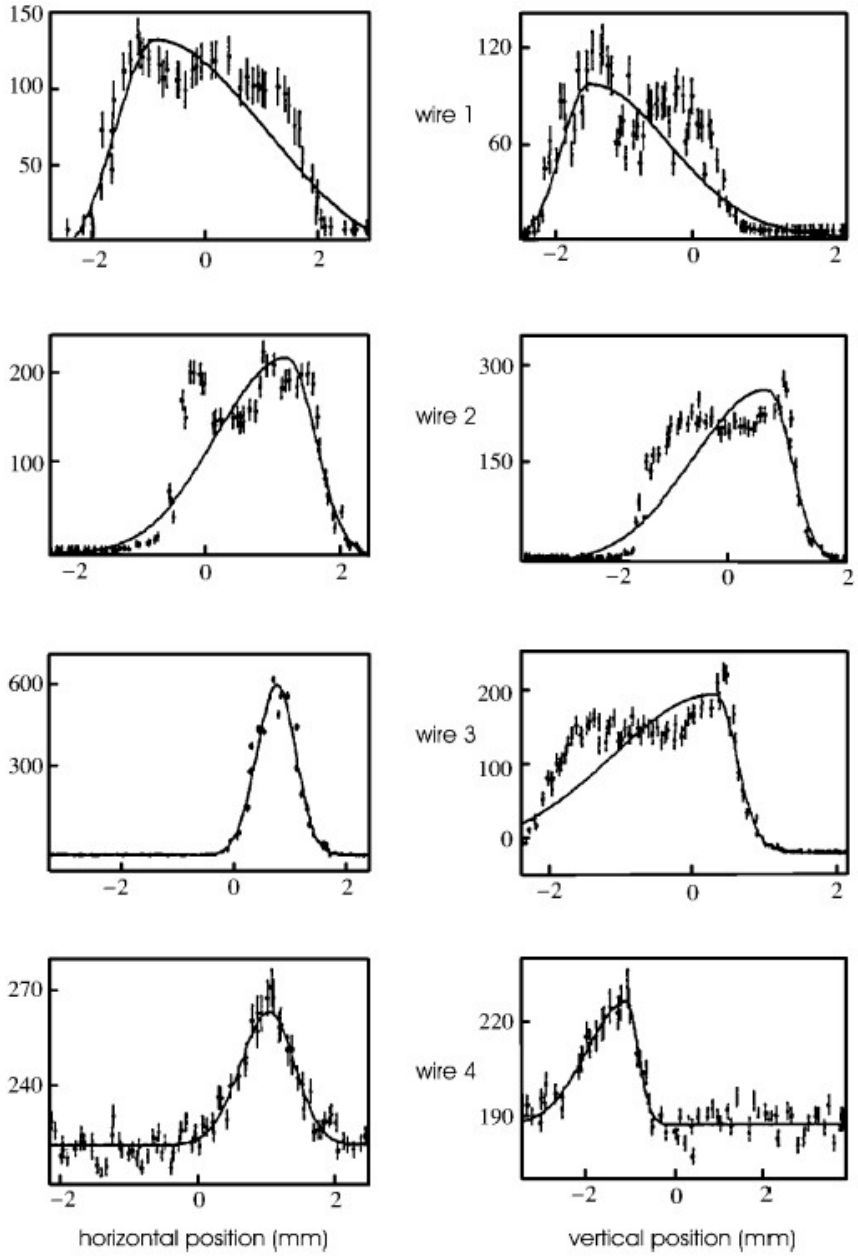

With methods I & II, the beam sizes may be measured using e.g. screens or wires

data: from the SLC main linac

Horizontal Beam Size Measurements
(scale in mm)

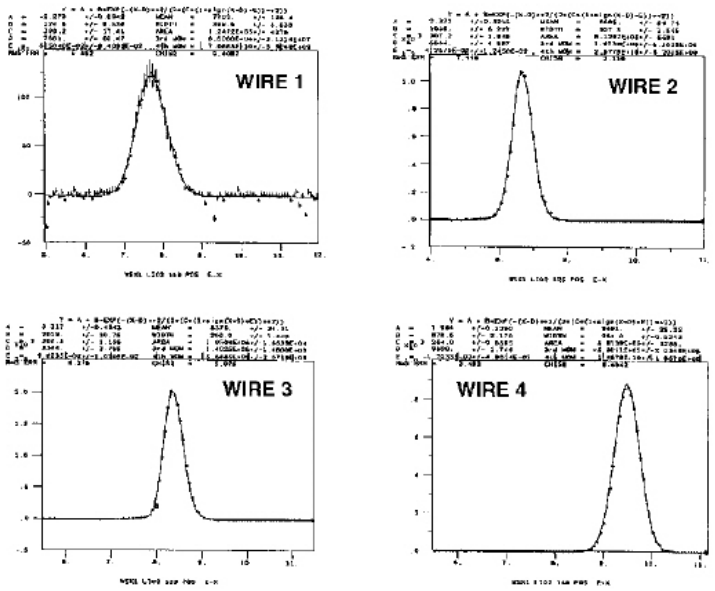

Vertical Beam Size Measurements
(scale in mm)

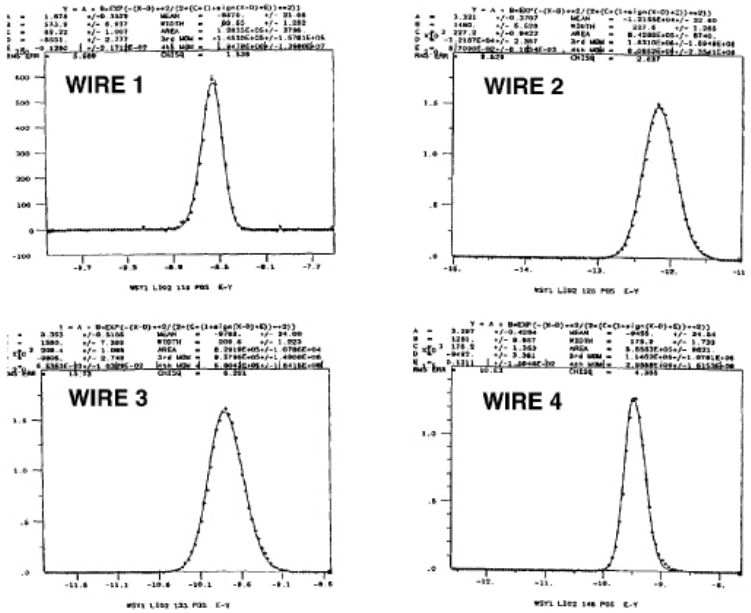

(scale in mm)

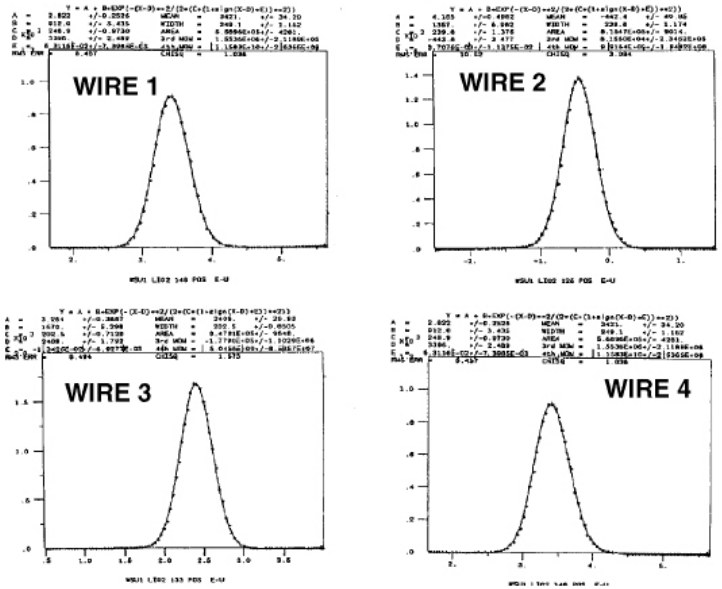

Four Dimensional Phase Space Analysis — LI02 ELEC 2.9E10/bunch

epsilon_x =	2.20	+-1.42E-02	epsilon_y =	1.89	+-1.72E-02
epsilon-b_x =	2.23	+-1.15E-02	epsilon-b_y =	1.95	+-2.05E-02
Bmag_x =	1.01	+-********	Bmag_y =	1.03	+-3.03E-03
Bmag_cos_x =	6.355E-02	+-1.13E-02	Bmag_cos_y =	0.248	+-1.12E-02
Bmag_sin_x =	0.152	+-1.50E-02	Bmag_sin_y =	3.112E-02	+-2.90E-02
beta_cos_x =	1.08	+-1.44E-02	beta_cos_y =	1.29	+-1.37E-02
beta_sin_x =	0.154	+-1.41E-02	beta_sin_y =	3.214E-02	+-3.00E-02
theta_1/deg =	-11.8	+-0.00E+00	theta_2/deg =	-12.6	+-0.00E+00
theta_3/deg =	-20.5	+-0.00E+00	theta_4/deg =	11.7	+-0.00E+00
tr(CC') =	0.245	+-0.00E+00	det C =	-0.114	+-0.00E+00
epsilon_1 =	2.13	+-0.00E+00	epsilon_2 =	1.71	+-0.00E+00
-det G+ =	3.265E-02	+-0.00E+00	psi+/deg =	-126.	+-0.00E+00
det G- =	0.128	+-0.00E+00	psi-/deg =	-89.4	+-0.00E+00
tr(BB') =	0.358	+-0.00E+00	det B =	0.104	+-0.00E+00

Emittance measurements using a (movable) Schottky monitor

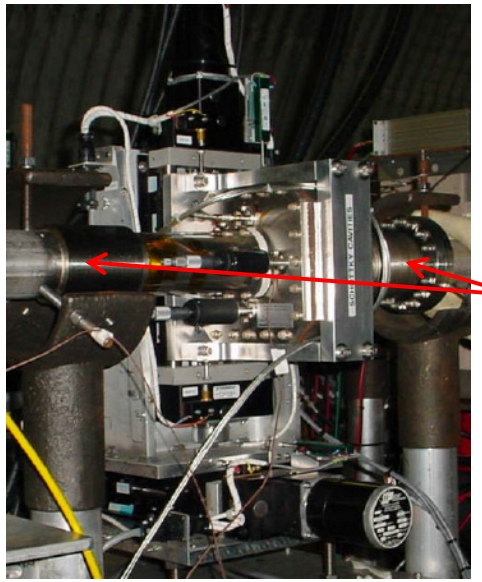

rms beam size, σ, is derived by taking the ratio of the power in the revolution line to the betatron lines. The position of the detector relative to X_0 is X.

$$\frac{P_0}{P_u + P_l} = \frac{(X - X_0)^2}{\sigma^2} + \frac{D^2\delta^2}{\sigma^2}$$

To measure, scan X and fit the resulting parabola to find σ, X_0, and the offset.

Note that the offset contains the dispersion.

Schottky and background spectra

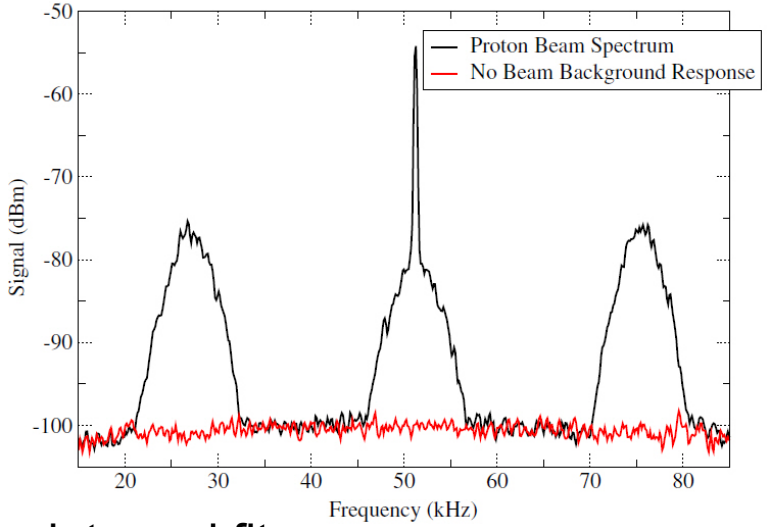

data and fits

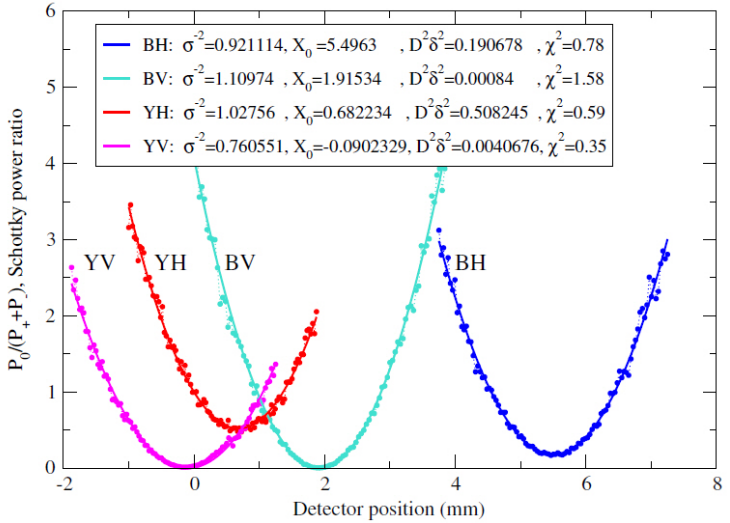

K.A. Brown et al, Measuring transverse beam emittance using a 2.07 GHz movable Schottky cavity at the Relativistic Heavy Ion Collider, Phys. Rev. ST Accel. Beams 12, 012801 (2009)

Betatron Tune, Q - definition

The stability of beams in a circular accelerator depends on the so-called “tune” of the accelerator, Q

oscillations about the ideal trajectory

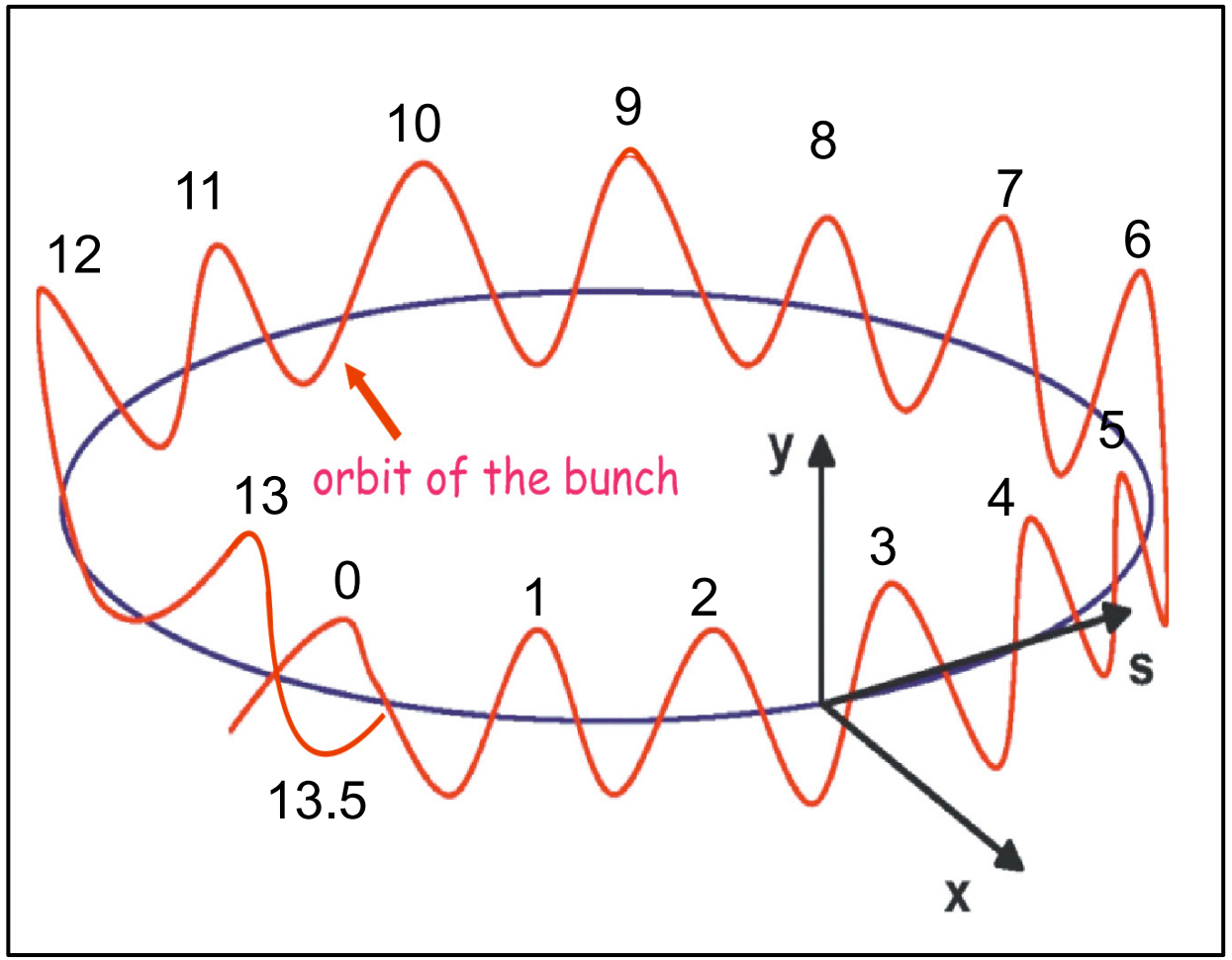

in this sketch, the tune is Q_y = 13.5 and Q = 0.5

Q is the number of oscillations made by a bunch in one revolution

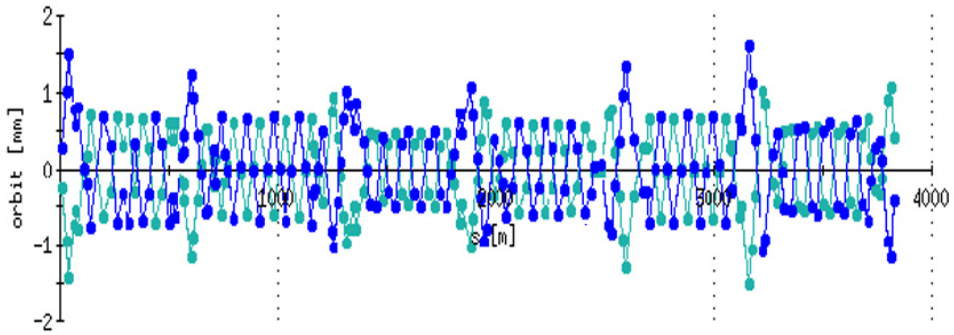

(easily determined by ‘counting’ oscillations)

the fractional tune Q dominates the beam dynamics (once the accelerator optics have been defined)

In an accelerator, resonances can occur if perturbations act on a bunch in synchronism with its oscillatory motion

The errors arise from imperfections (or misalignments) of the accelerator's magnets

resonance condition

$$m\,Q_x + n\,Q_y = p$$

(m, n, and p are integers)

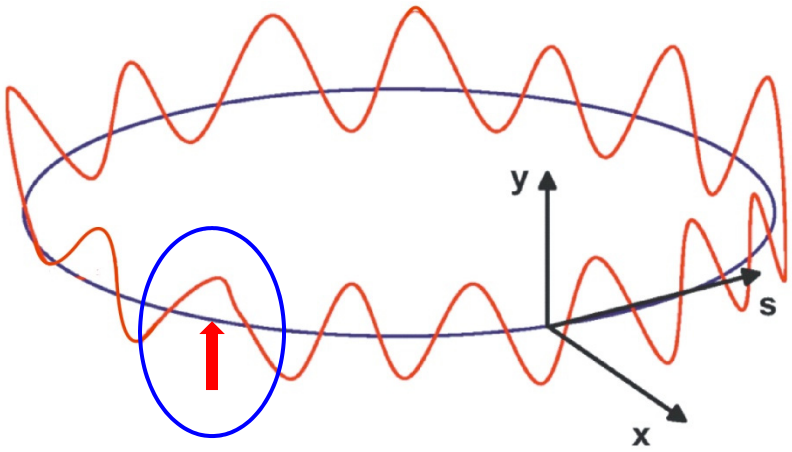

first order (strongest)

m = 0, n = 1, p = 1

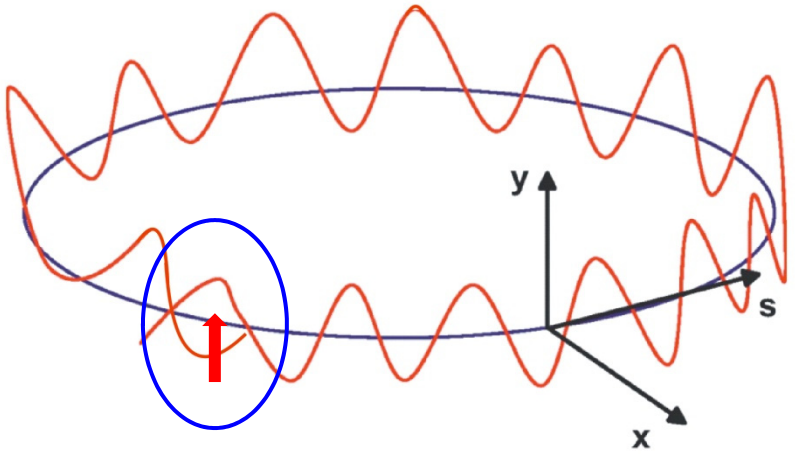

second order

m = 0, n = 2, p = 1

Tune diagram

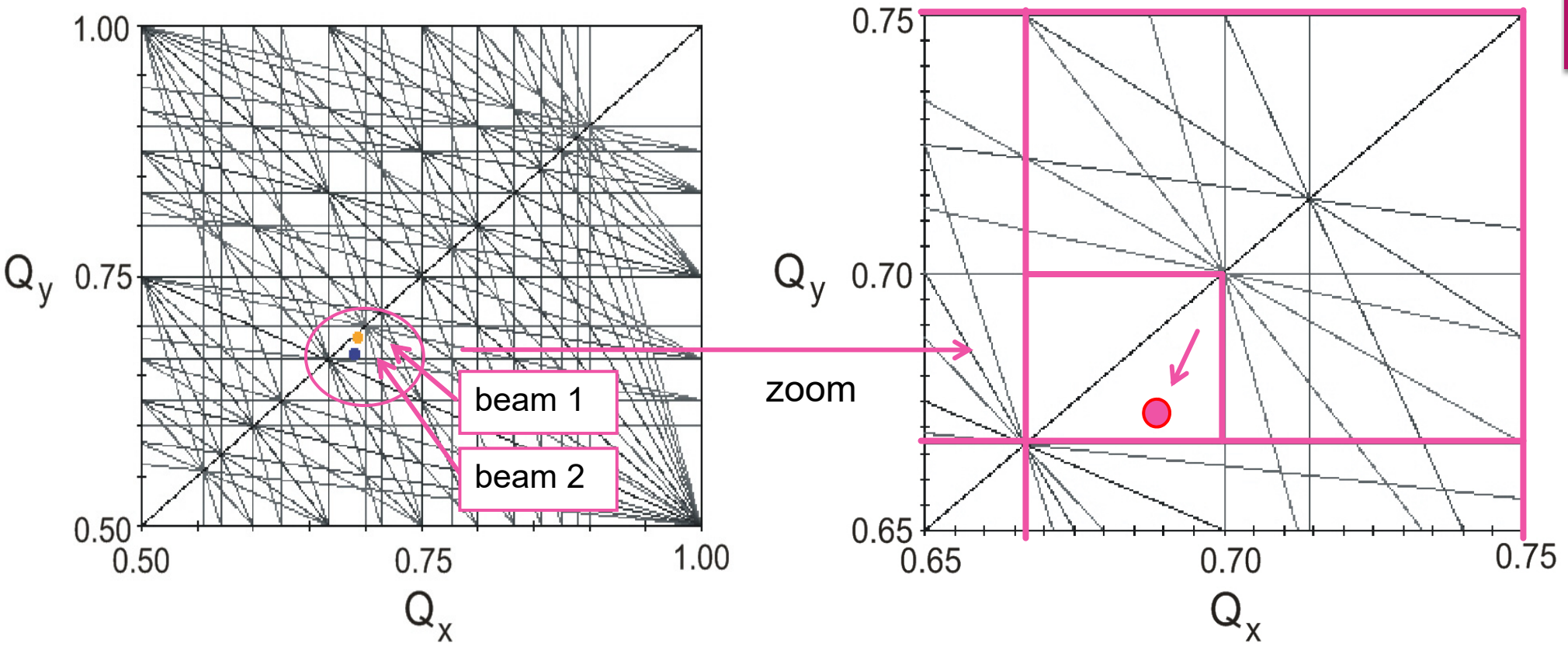

colliders tend to operate along the diagonal

At RHIC ‘operating point’ bounded by strong 3rd and 4th order resonances

for polarized proton operation, the resonance at 0.70 is critical

the operating point is moved during acceleration

Betatron Tune, Q - measurement

Two general approaches:

FFTs of turn-by-turn Beam Position Monitor measurements
challenge: sensitivity
using dedicated system optimized for beam oscillation detection; for example direct diode detection

---

envelop demodulation with diode peak detector

DC block

signal enhancement using opposite electrode

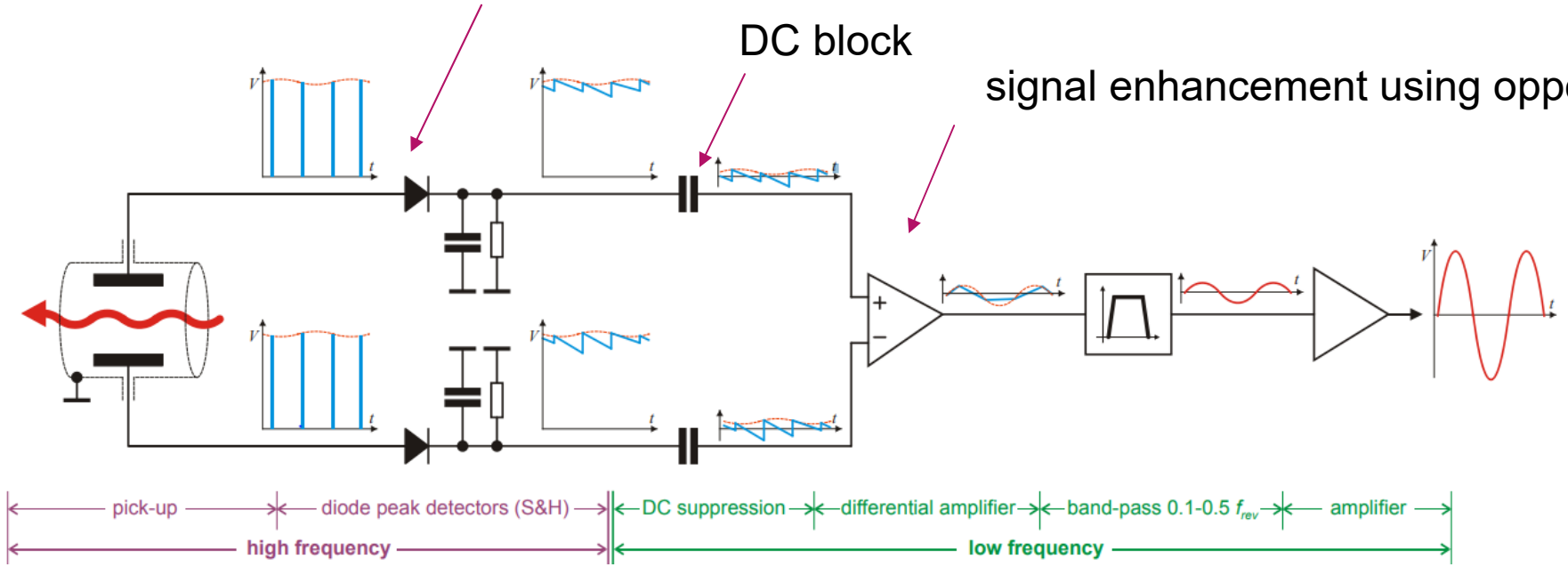

From M. Gasior, R. Jones, T. Lefevre, H. Schmickler, K. Wittenburg https://arxiv.org/ftp/arxiv/papers/1601/1601.04907.pdf
also M. Gasior, R. Jones, T. Lefevre The Principle and First Results of Betatron Tune Measurement by Direct Diode Detection (2005)

Measurement of Beta Functions

Multiple methods including

a) measurement at a single quadrupole

measure tune shift ΔQ induced by quadrupole strength change ΔK → b at this quadrupole

$$\beta \approx \frac{4\pi\Delta Q}{\Delta K}$$

assumes $\cot(2\pi Q_0) \leq 1$

$\Delta Q << 1$

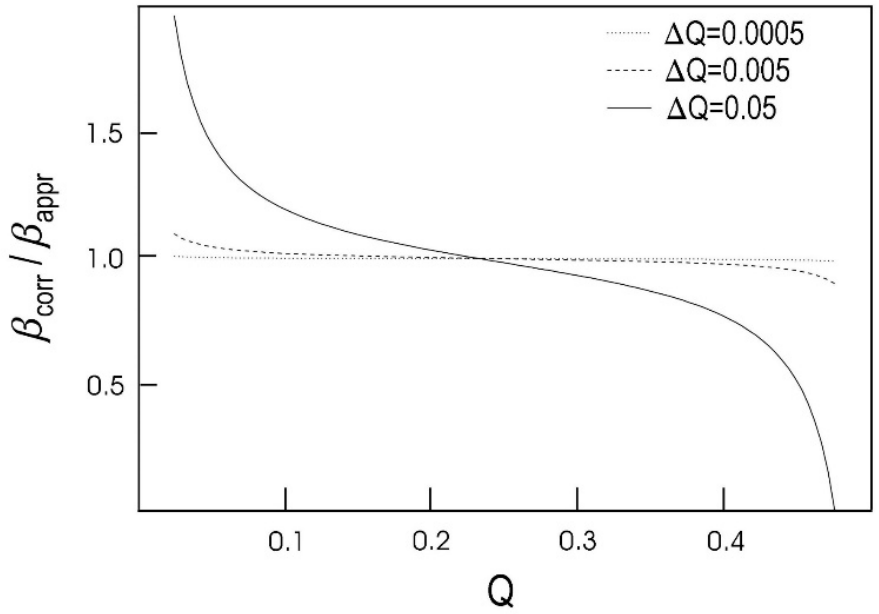

b) Measurement at multiple BPMs

transport matrix from *i* to *f*:

$$\begin{pmatrix} \sqrt{\beta_f/\beta_i}\left(\cos\phi_{fi} + \alpha_i \sin\phi_{fi}\right) & \sqrt{\beta_f\beta_i}\sin\phi_{fi} \\ -\frac{1+\alpha_i\alpha_f}{\sqrt{\beta_f\beta_i}}\sin\phi_{fi} + \frac{\alpha_i - \alpha_f}{\sqrt{\beta_f\beta_i}}\cos\phi_{fi} & \sqrt{\beta_i/\beta_f}\left(\cos\phi_{fi} - \alpha_f \sin\phi_{fi}\right) \end{pmatrix}$$

$$= \begin{pmatrix} R_{11} & R_{12} \\ R_{21} & R_{22} \end{pmatrix}$$

the 1st row can be rewritten as $\tan\phi_{fi} = \frac{R_{12}^{fi}}{R_{11}^{fi}\beta(s_i) - R_{12}^{fi}\alpha(s_i)}$

R_{11}, R_{12} can be calculated (over short sections)
ϕ_{fi} is measured ⟶ 2 unknowns β_i, α_i

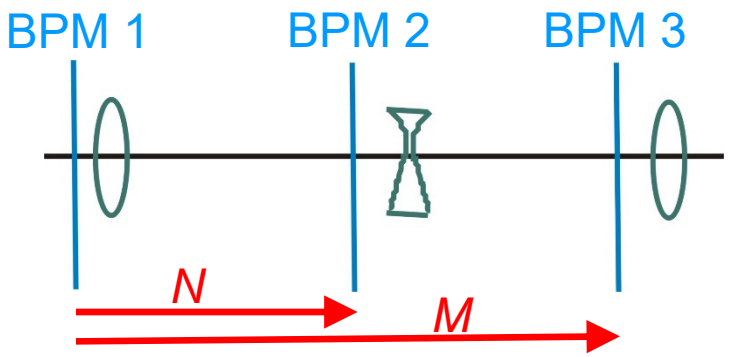

$$M = \begin{pmatrix} m_{11} & m_{12} \\ m_{21} & m_{22} \end{pmatrix}, \quad N = \begin{pmatrix} n_{11} & n_{12} \\ n_{21} & n_{22} \end{pmatrix}$$

combine to eliminate $\alpha(s_i)$ in previous equation:

$$\beta(s_i) = \frac{\frac{1}{\tan\phi_{21}} - \frac{1}{\tan\phi_{31}}}{\frac{m_{11}}{m_{12}} - \frac{n_{11}}{n_{12}}}$$

$$\alpha(s_i) = \frac{\frac{n_{11}}{n_{12}\tan\phi_{21}} - \frac{m_{11}}{m_{12}\tan\phi_{31}}}{\frac{m_{11}}{m_{12}} - \frac{n_{11}}{n_{12}}}$$

independent of BPM calibration

$$x_{km} = A_k \cos(2\pi Q m + \phi_{0k})$$

k = BPM number
m = turn number

betatron phase at k^{th} BPM

$$C_k = \sum_{m=1}^{N} x_{km} \cos(2\pi Q m)$$

$$S_k = \sum_{m=1}^{N} x_{km} \sin(2\pi Q m)$$

$$\phi_{0k} \approx -\tan^{-1}\left(\frac{S_k}{C_k}\right)$$

P. Castro, PhD Thesis

Beta function measurements

LHC β -beat measurements
with β*=40 cm

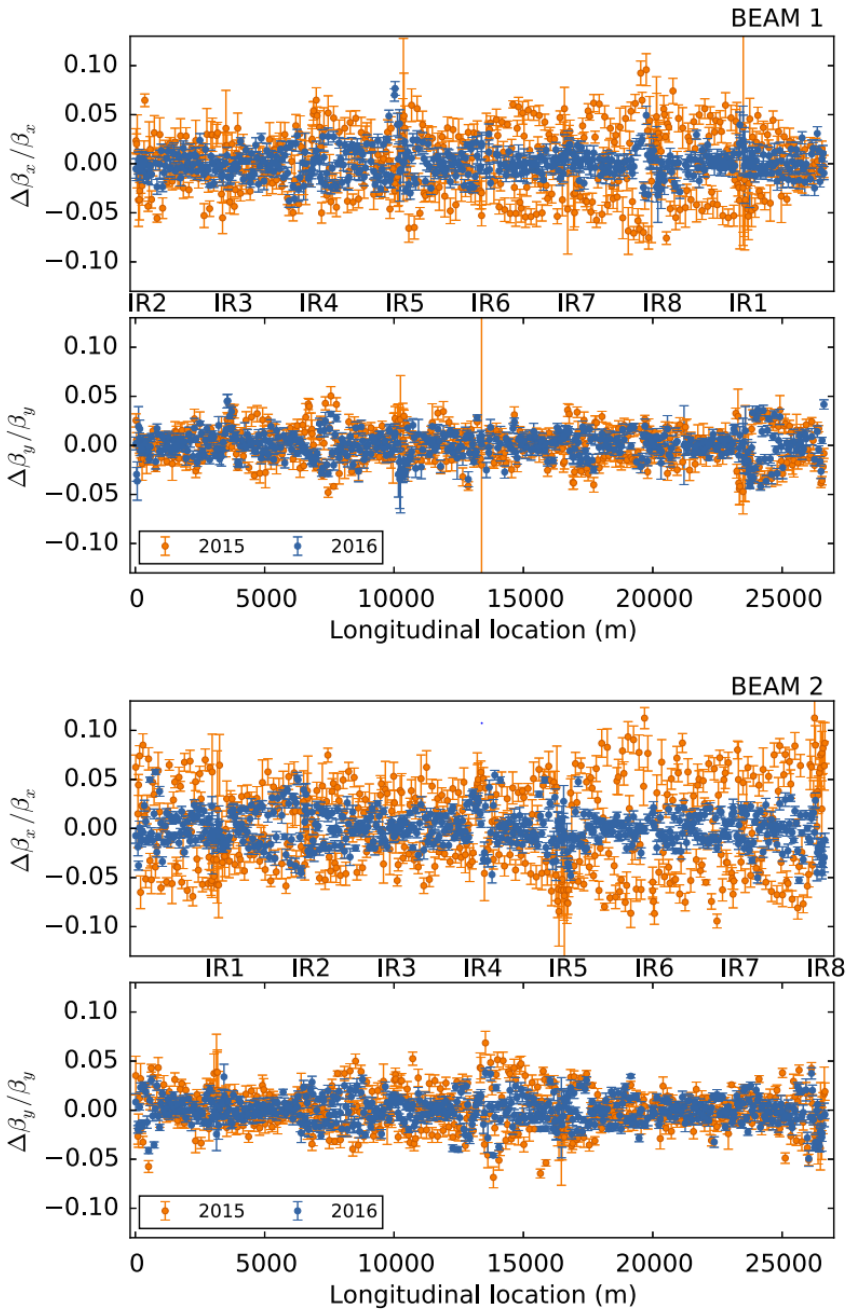

LHC optics commissioning: A journey towards 1% optics control, T. Persson et al, PRAB 20, 061002 (2017)

Beta Function Measurements during Acceleration

- motivation: improve understanding of emittance evolution during acceleration
  correct optics during acceleration cycle
- strategy: orchestrate data acquisitions and data delivery using interleaved
  average orbit BPM measurements (for orbit feedback) and
  turn-by-turn BPM measurements (for optics measurements)

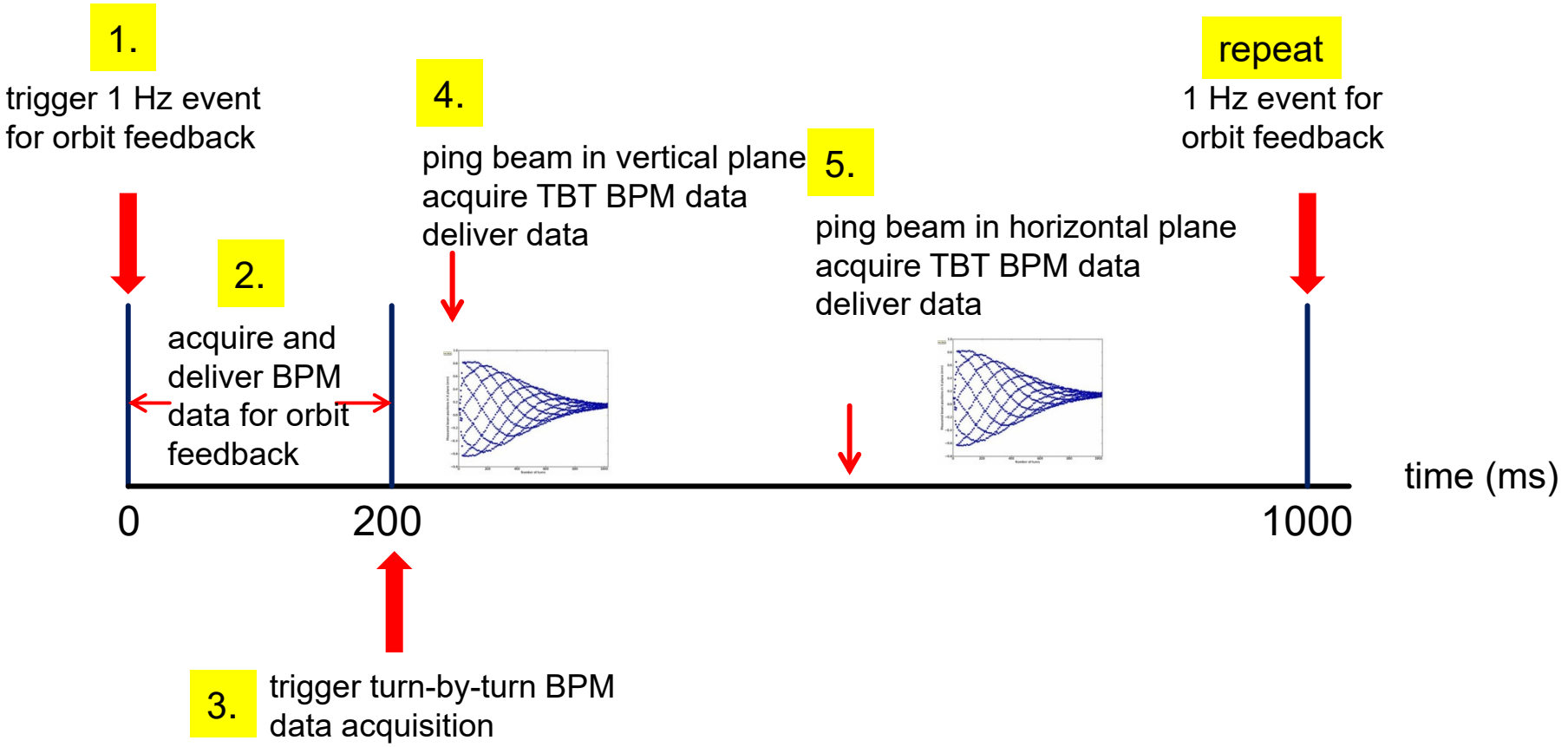

Beta Function Measurement

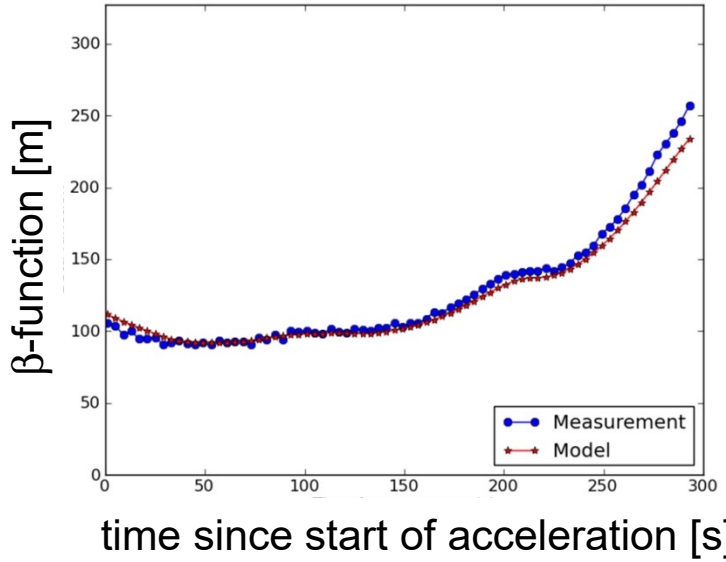

model versus measured β_y at IPM

Beta Function Correction

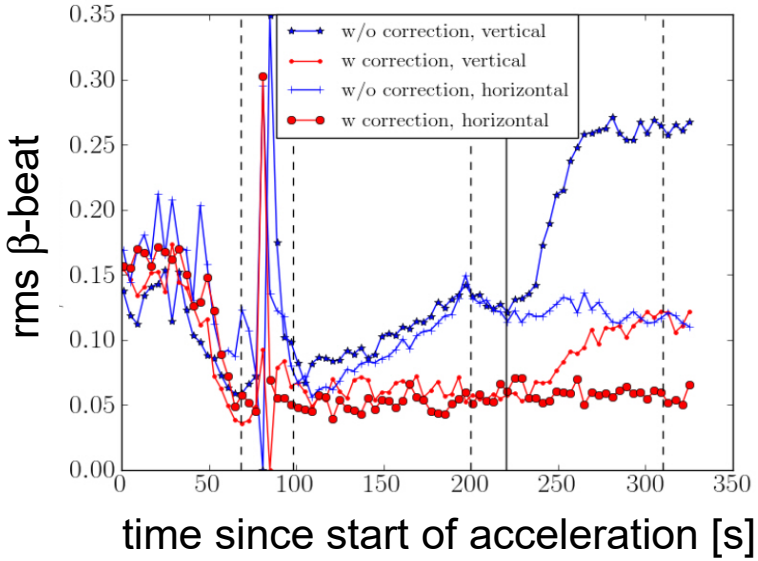

rms β-beats before and after correction

M. Minty et al, Measurement of beam optics during acceleration in RHIC, NAPAC13
C. Liu et al, Optics measurement and correction during acceleration with beta-squeeze in RHIC, IPAC15

Coupling

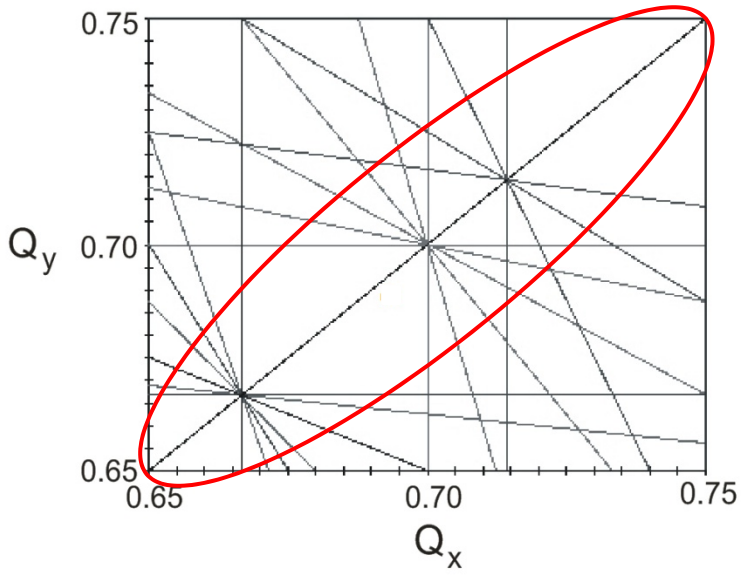

resonance-free region has $Q_x \sim Q_y$
… precisely where coupling effects are strongest

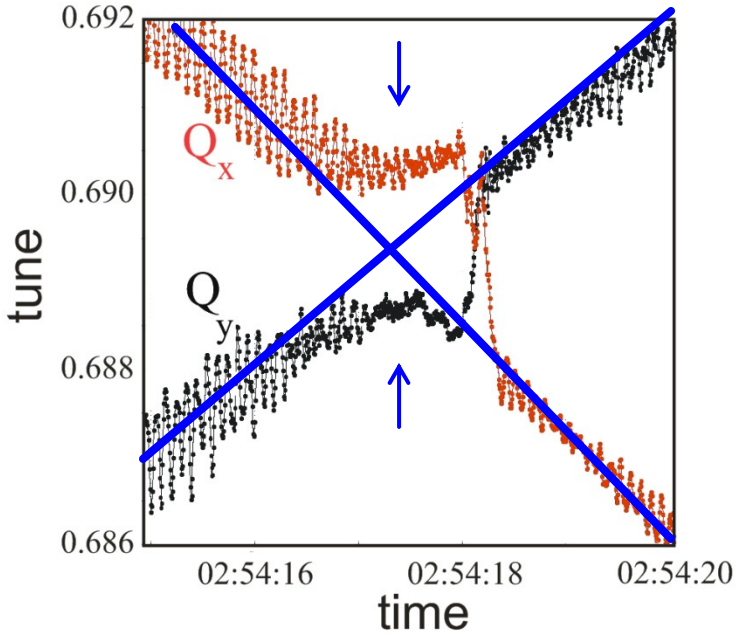

with $Q_x \sim Q_y$ and nonzero coupling, beam control in one plane affects the other and produces unexpected results

coupling measurement: distance of closest approach

coupling measurement

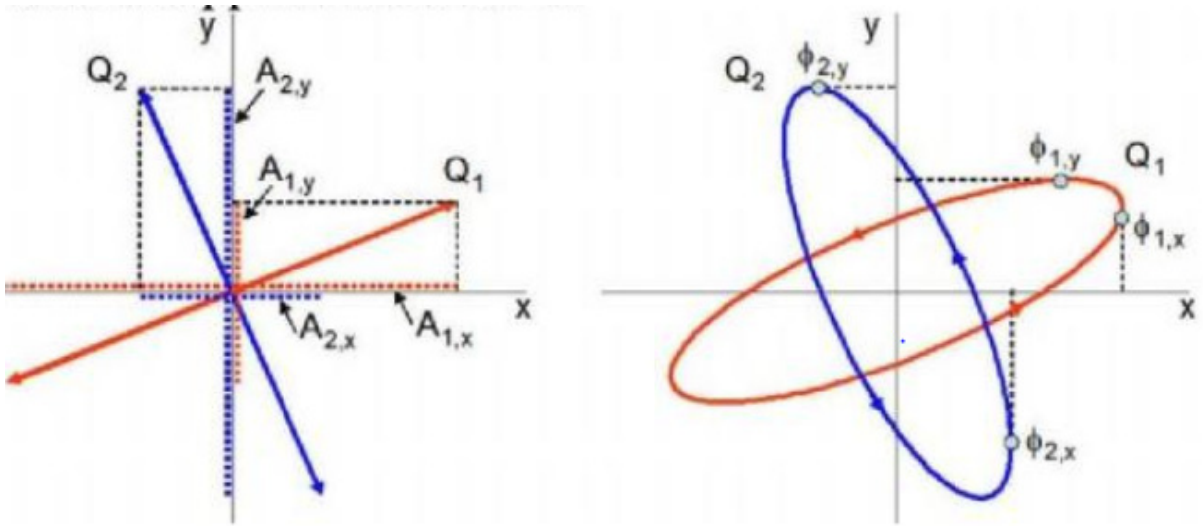

coupling coefficients

$$|C^-| = \frac{2\sqrt{r_1 r_2}|Q_x - Q_y|}{1 + r_1 r_2},$$

$$\Delta = \frac{|Q_x - Q_y|(1 - r_1 r_2)}{1 + r_1 r_2},$$

with $r_1 = \frac{\tilde{A}_{1y}}{\tilde{A}_{1x}}$ and $r_2 = \frac{\tilde{A}_{2x}}{\tilde{A}_{2y}}$

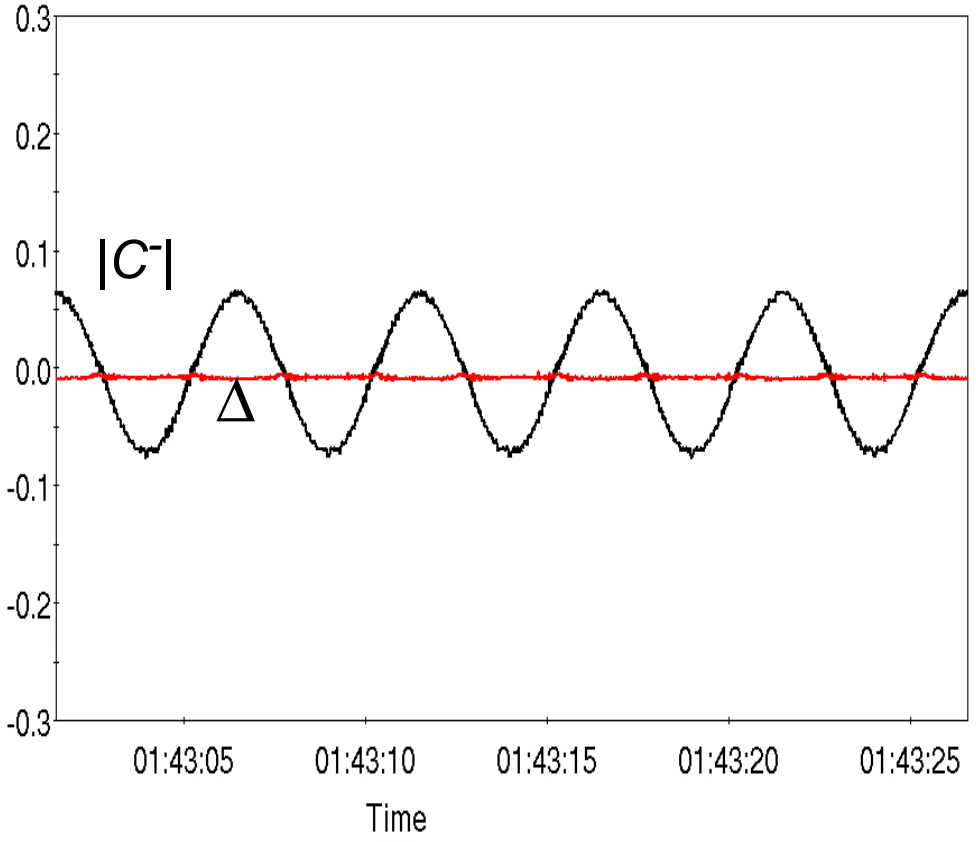

Chromaticity, definitions

normalized $\xi = \dfrac{\Delta Q / Q}{\Delta p / p}$ unnormalized $Q' = \dfrac{\Delta Q}{\Delta p / p}$

relation $\xi = Q' / Q$

- chromaticity describes the change of focusing with particle energy
- small chromaticity: desired to minimize tune spread induced by finite energy spread and to
- reduce synchro-betatron coupling (maximize dynamic aperture)
- set slightly positive (above transition energy) – avoid head-tail instability
- large positive chromaticity is often employed to damp instabilities (ESRF, Tevatron, SPS,…)

Measurement of Chromaticity using Betatron Tune

Measure change in betatron tune at different rf frequencies

$$Q'_{x,y} = \frac{\Delta Q_{x,y}}{\Delta p / p}$$

$$= -\left(\alpha_C - \frac{1}{\gamma^2}\right)\frac{\Delta Q_{x,y}}{\Delta f_{rf} / f_{rf}}$$

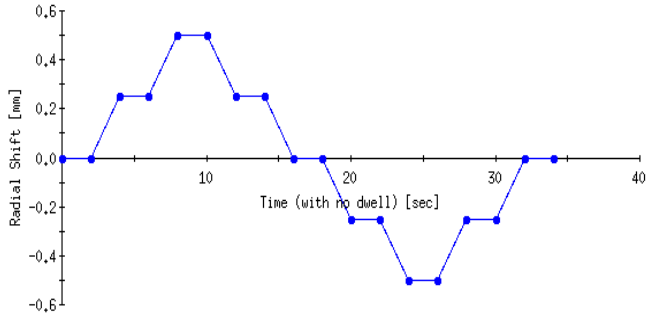

horizontal position vs time as rf frequency is changed

chromaticity measurement

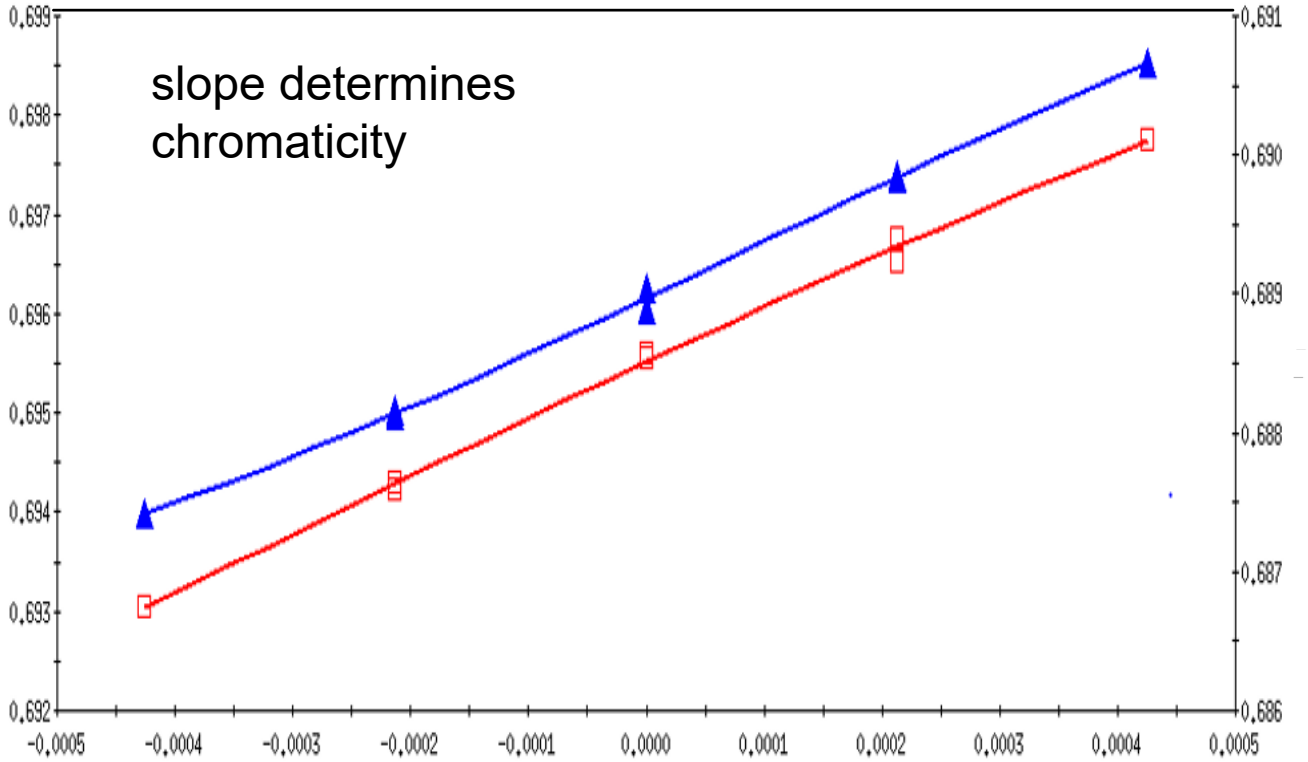

Chromaticity Feedback

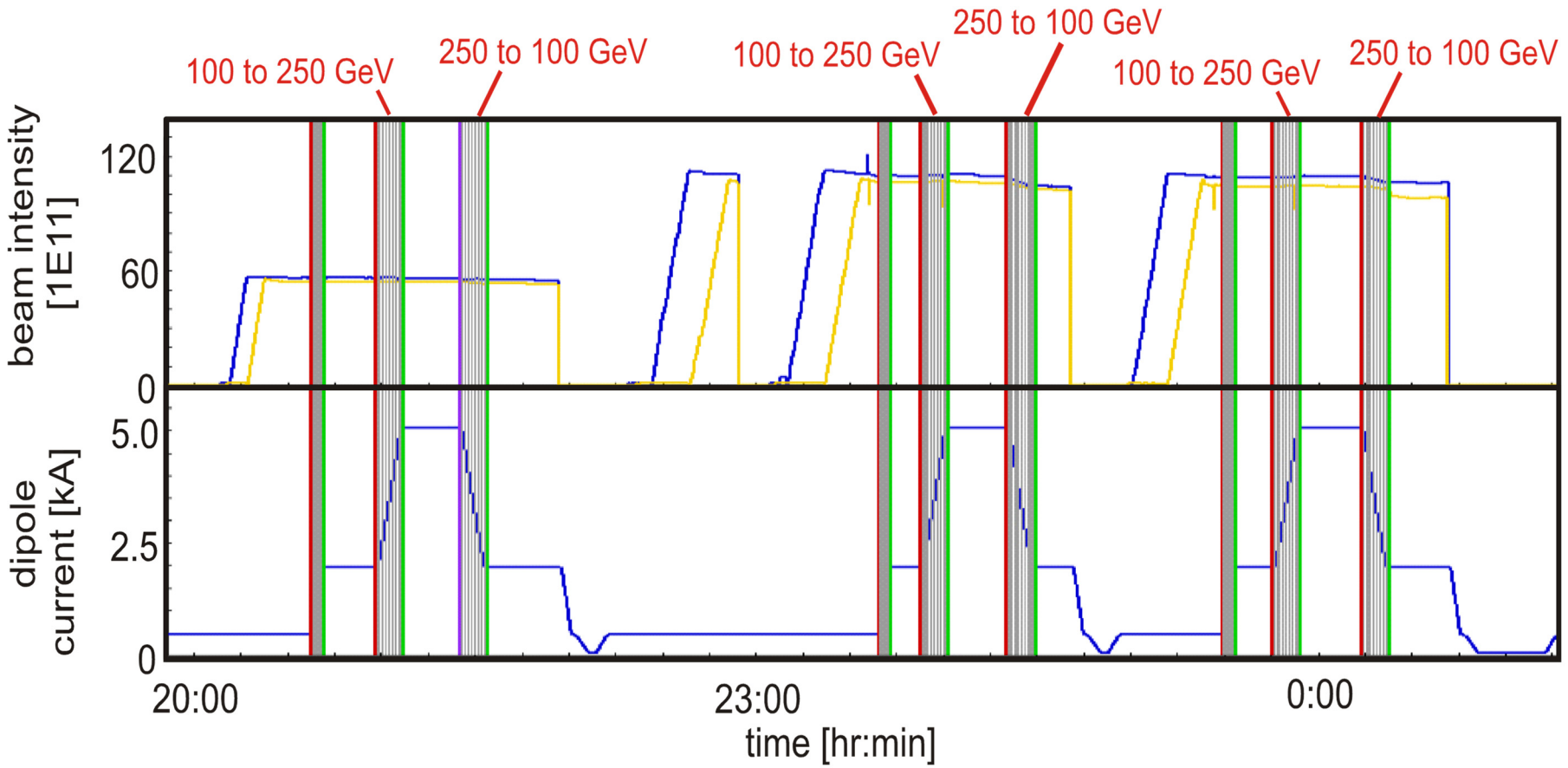

- rf frequency sinusoidially modulated with zero crossings for orbit feedback measurements
- action of tune/coupling feedback used to infer chromaticity
- application of all feedback loops (with high-fidelity data inputs) allowed for acceleration *and deceleration* of particle beams in superconducting accelerator

Recent Developments and Future Challenges

- Electron Lenses
- Bunched Beam Electron Cooling

Common theme: detection and relative alignment of co-propagating beams

Electron Lenses for head-on beam-beam compensation

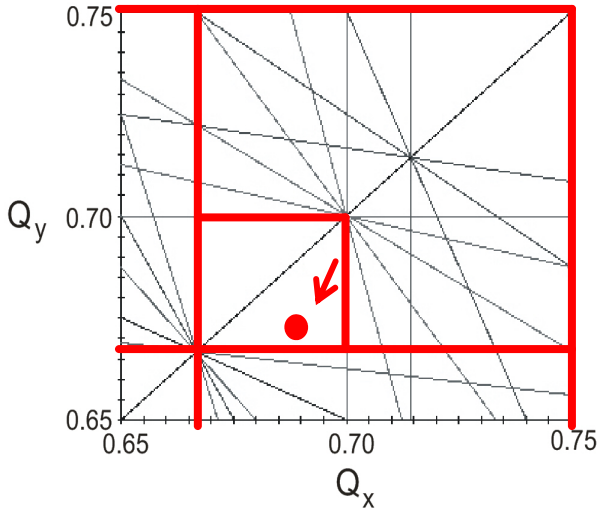

Motivation:

- Ultimate collider performance limited by beam-beam focusing
- Electron lenses compensate the beam-beam space charge forces

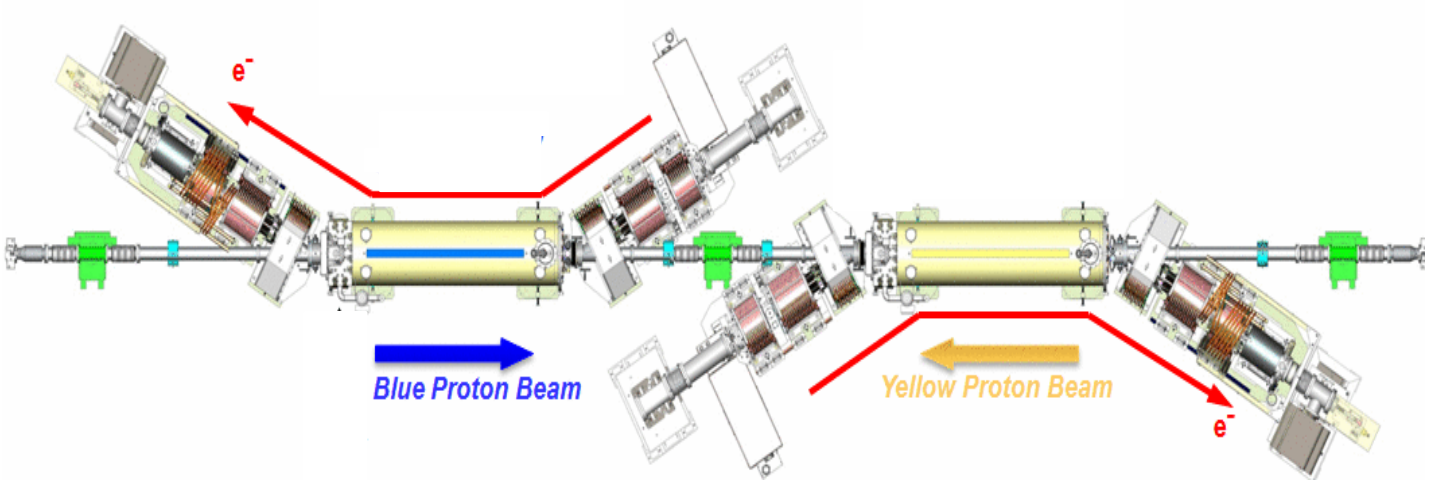

Layout of the electron lenses in the BNL collider

Challenge: ensuring overlap (collinear trajectories) of proton and electron beams

W. Fischer et al, Operational head-on beam-beam compensation with electron lenses in the Relativistic Heavy Ion Collider, Phys. Rev. Lett. **115**, 264801 (2015)

Electron Back-Scattering Detector

Low-energy electrons acquire high energies in small impact parameter Coulomb scattering collisions with relativistic ions

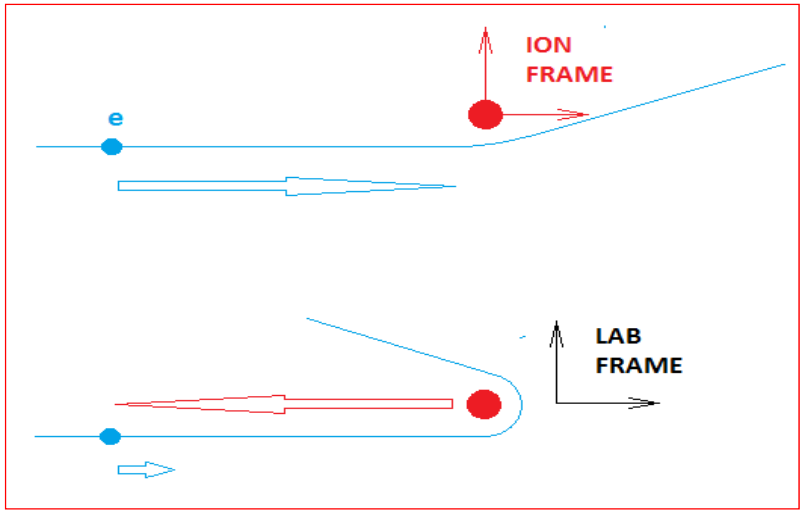

Small deflections in the ion frame lead to large deflections in the lab.

The classical Rutherford scattering equation with quantum and recoil corrections used to calculate the cross sections in the ion frame of reference.

p = momentum E = energy θ = angle of the electron in the ion frame

$$\frac{d\sigma}{d\Omega} = \frac{Z^2}{4}\left(\frac{e^2}{E}\right)^2 \frac{1}{sin^4(\theta/2)} \times \left[1 - \left(\frac{pc}{E}\right)^2 sin^2\frac{\theta}{2}\right] \times \left[1 + \frac{2E\,sin^2(\theta/2)}{M_p c^2}\right]^{-1} \times \left[1 - \frac{q^2 \tan^2(\theta/2)}{2M_p^2}\right]$$

Rutherford | Quantum corr. | Recoil corr. | Magnetic moment corr.

P. Thieberger et al, High energy Coulomb-scattered electrons for relativistic particle beam diagnostics, PRAB **19**, 041002 (2016)

Electron Back-Scattering Detector for Electron-Proton Alignment

simulated trajectories

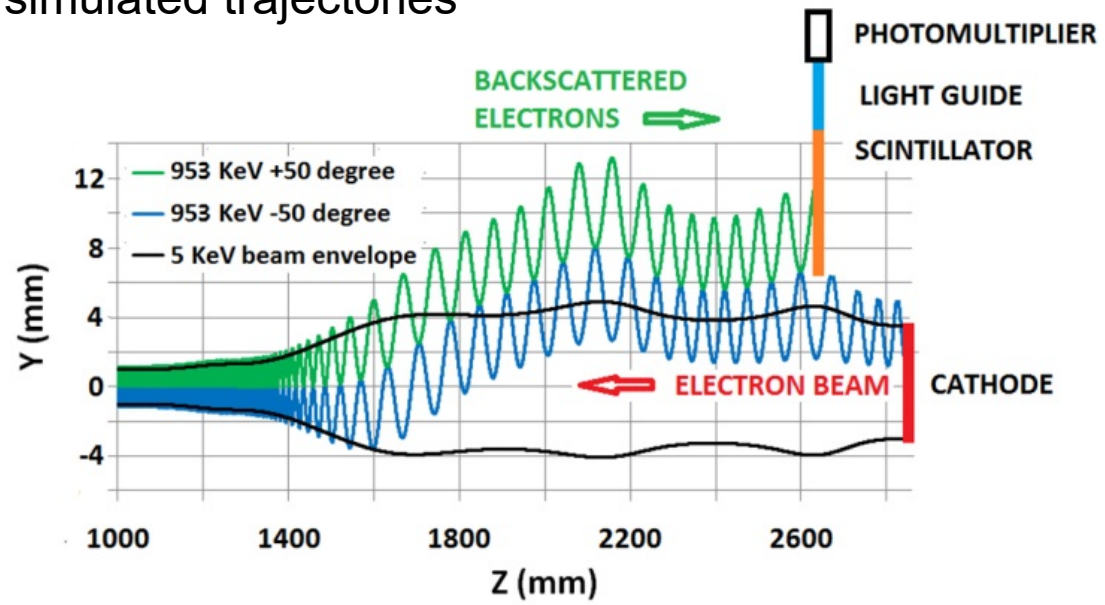

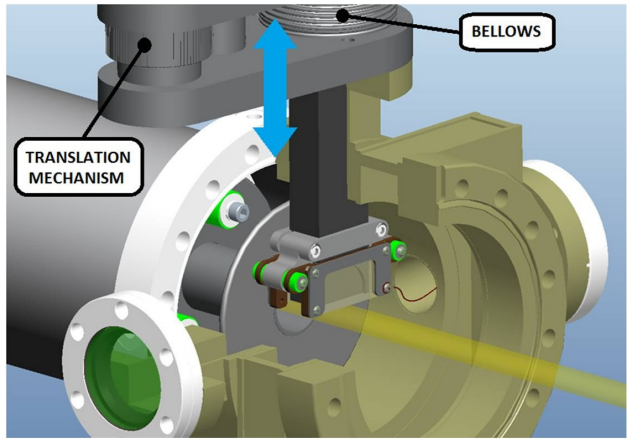

Thin (0.1mm) Titanium vacuum window (with < 0.1 MeV dE/E) for 0.5 to 10 MeV electrons

In-air scintillator and motion control

data

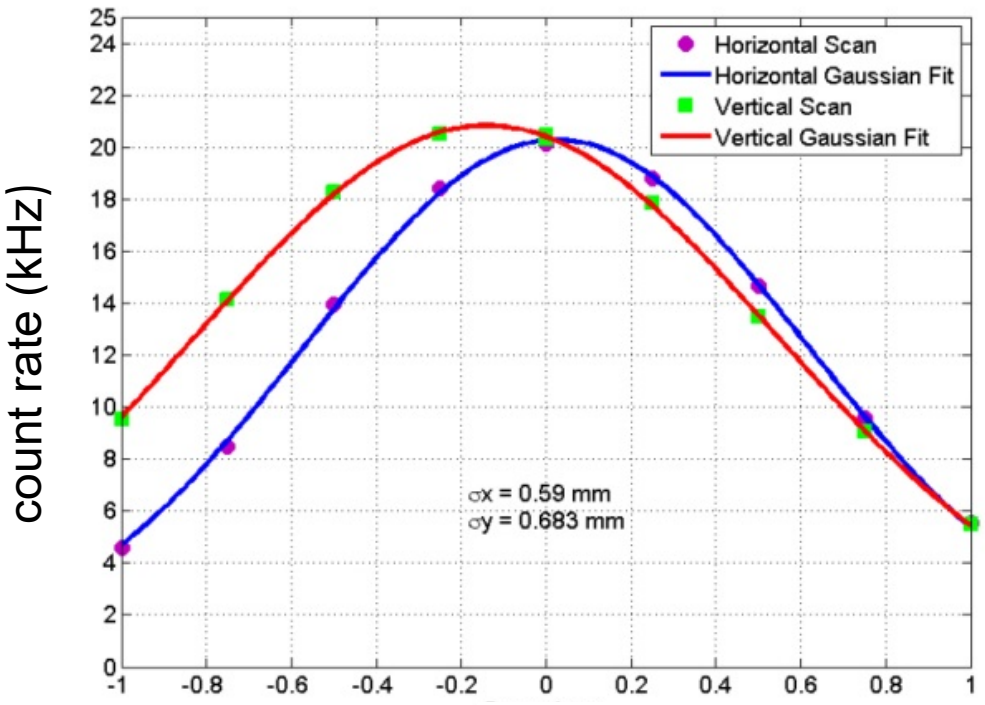

Recent applications for ‘hollow’ beam alignment (not shown)

Bunched-Beam Electron Cooling

- Based on RF acceleration of bunched electron beam (all previous coolers used DC beams)
- Developed for ongoing program at BNL (QCD critical point search)
- Required for high-energy electron cooling; possible applications for a future accelerators (e.g. EIC)

Instrumentation Challenges

- Trajectories of electrons and to-be-cooled beams must be aligned to high accuracy
- Relative velocities of electrons and to-be-cooled beams must be equal to high accuracy (~ 5E-4)

Instrumentation Developments

- Dual frequency BPM electronics
- Radiative recombination monitor
- Systematic approach to relative beam energy matching

THZBA5 - First Electron Cooling of Hadron Beams Using a Bunched Electron Beam, A. Fedotov, et al

Layout of the electron accelerator for electron cooling in RHIC

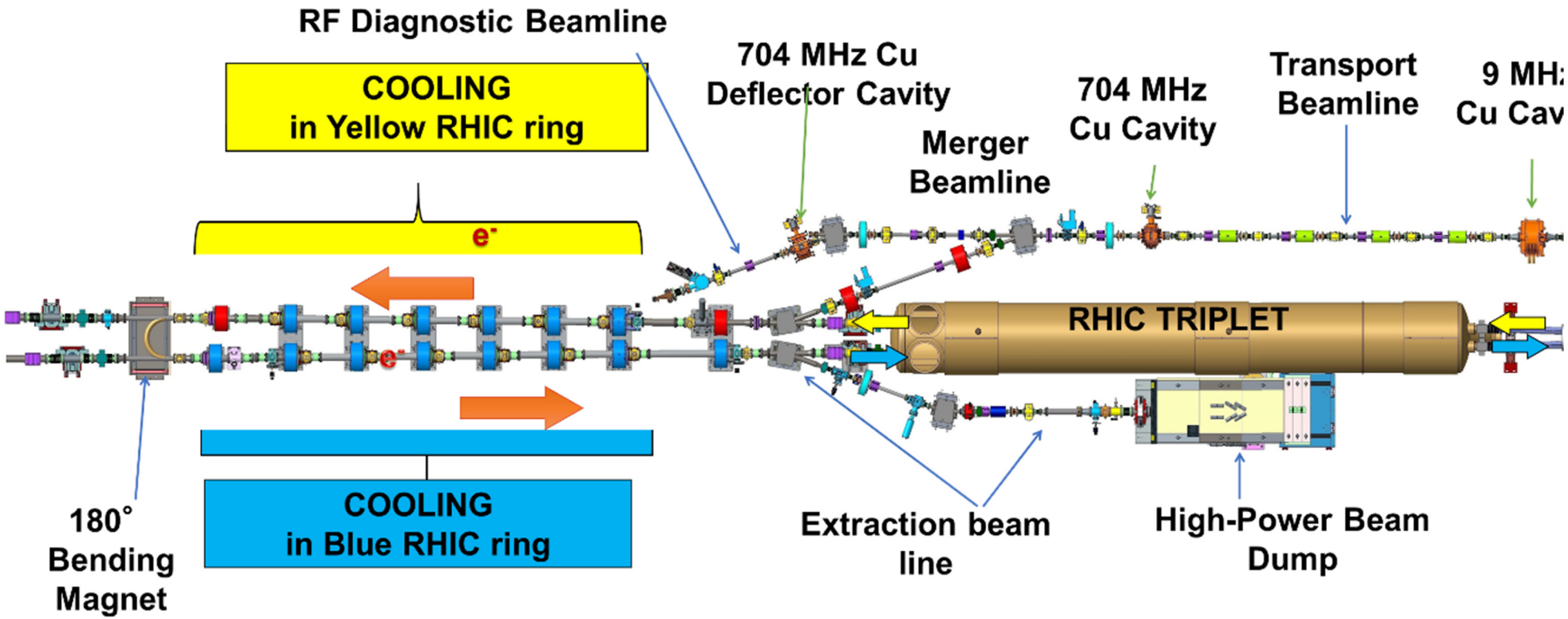

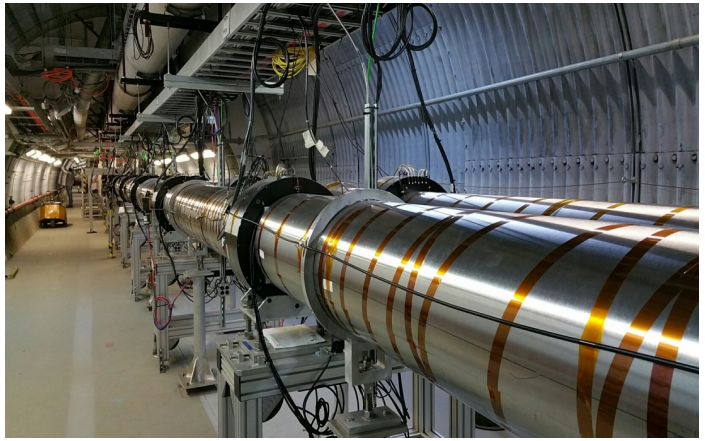

(Select) challenging electron beam requirements

RMS energy spread	< 5e-4
RMS angular spread	<150 urad

TUZBA1 - Commissioning of the Electron Accelerator LEReC for Bunch Beam Cooling, D. Kayran, et al

LEReC Beam Structure in the Cooling Section

Electrons

f =704 MHz
30-bunches at 9 MHz

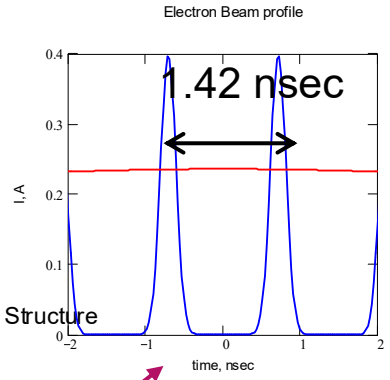

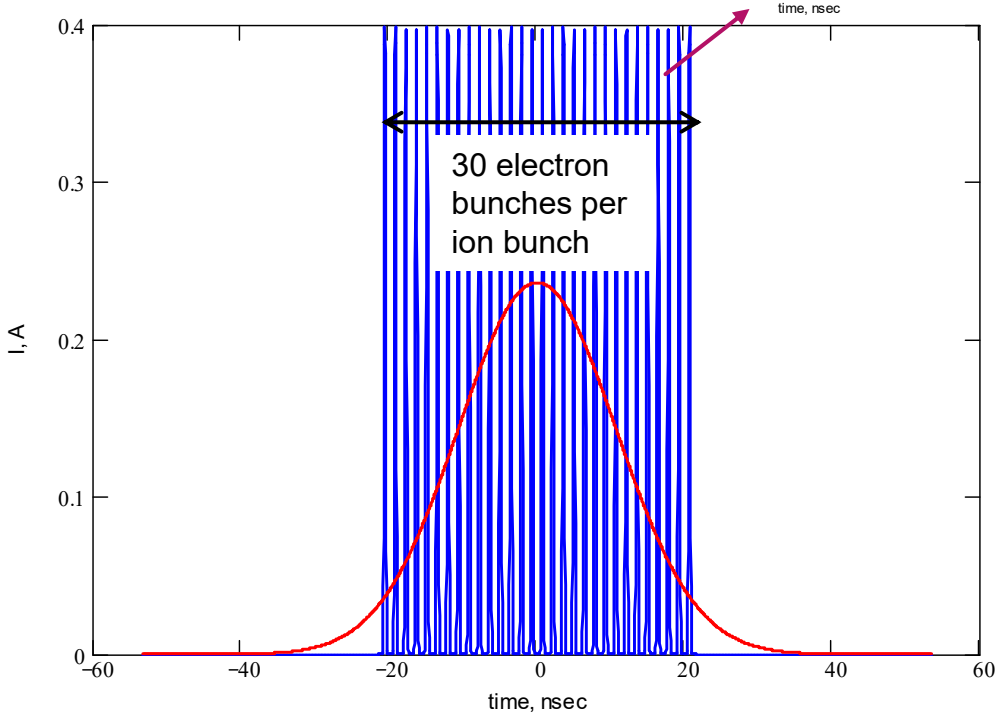

Ions

f = 9 MHz

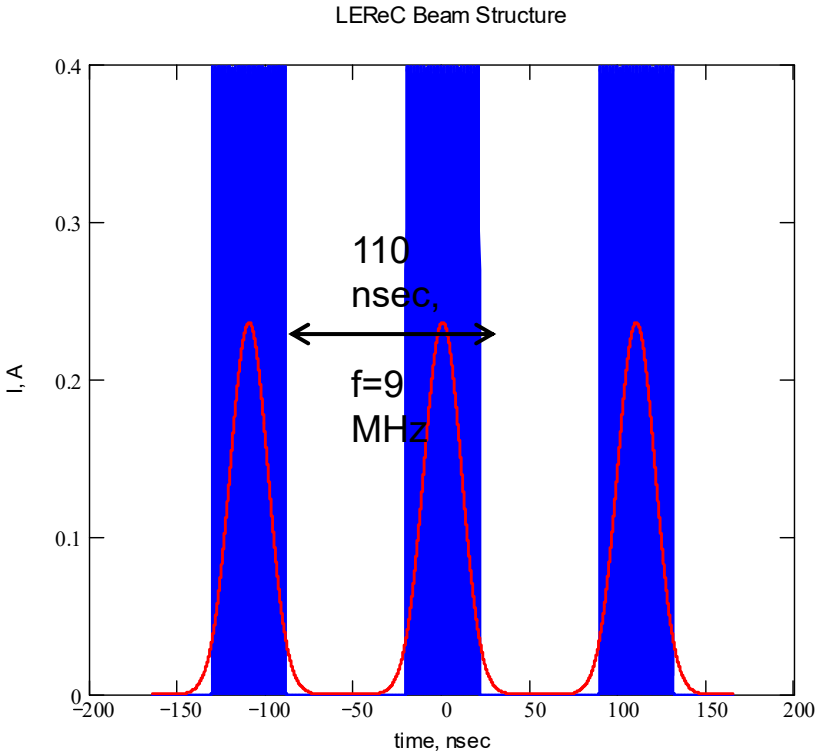

Electron-Ion Trajectory Overlap: Button BPMs + Dual Frequency BPM Electronics

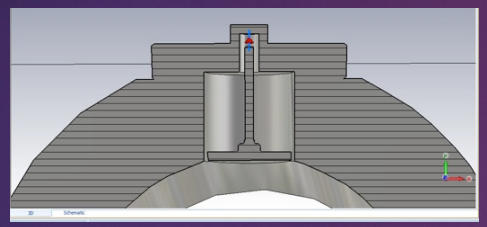

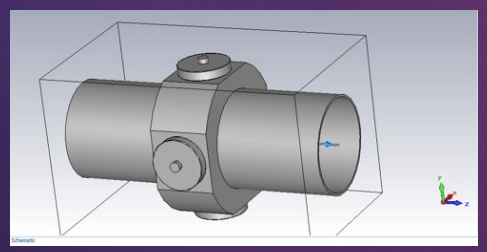

- each BPM Pickup signal is split into two different electronics
  - low-pass (10MHz) sensitive to 9MHz bunching of e- and ion beam
  - band-pass (704MHz) sensitive to e- beam only

- 9MHz used to align ion and electron beam
  - with ion beam only can use drift section for BBA
  - detects combined effect of ion and electron beams

- 704MHz only responds to electrons (even with ions present)
  - can monitor effects of ion beam on e- beam
  - can track drifts in electron beam while cooling

LEReC /RHIC BPM Data Using Dual Frequency Electronics

9MHz e- or Ion Signal (4 Bunches)

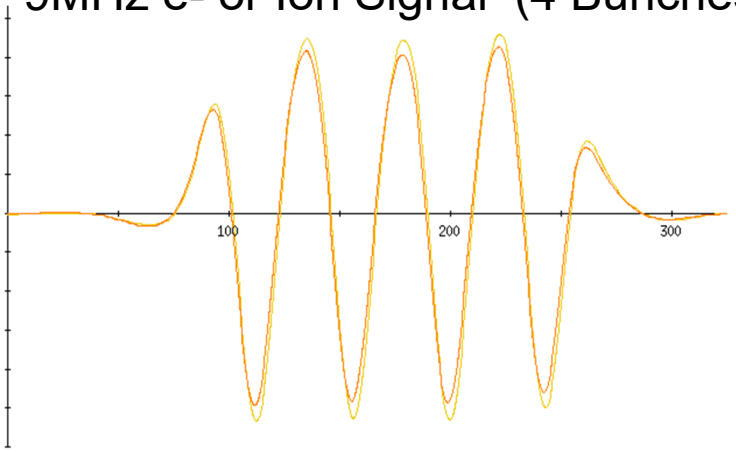

704MHz e- Signal (4 Bunches)

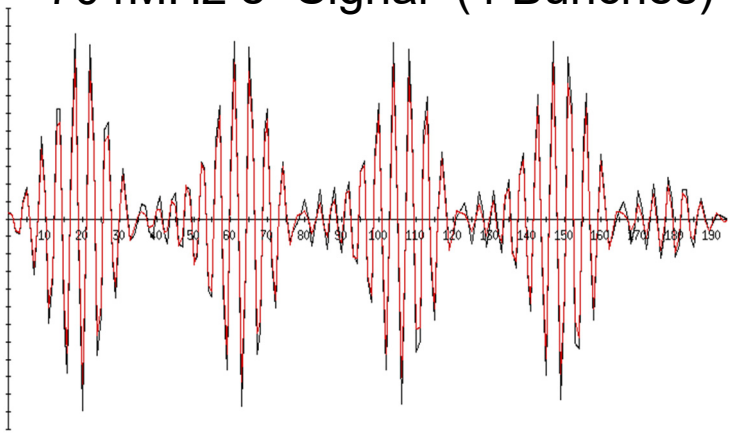

Ion intensity

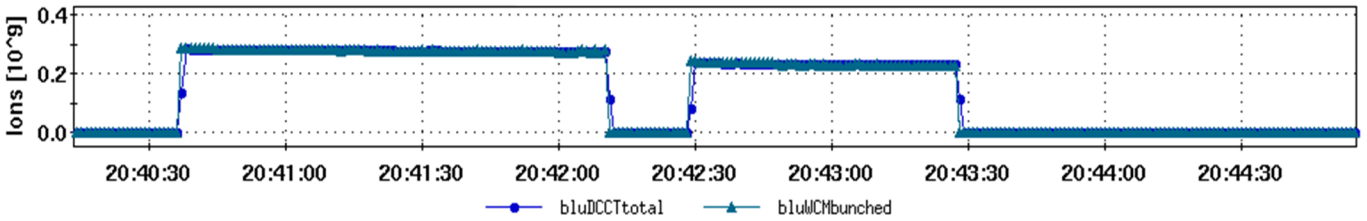

9MHz positions – detects both beams

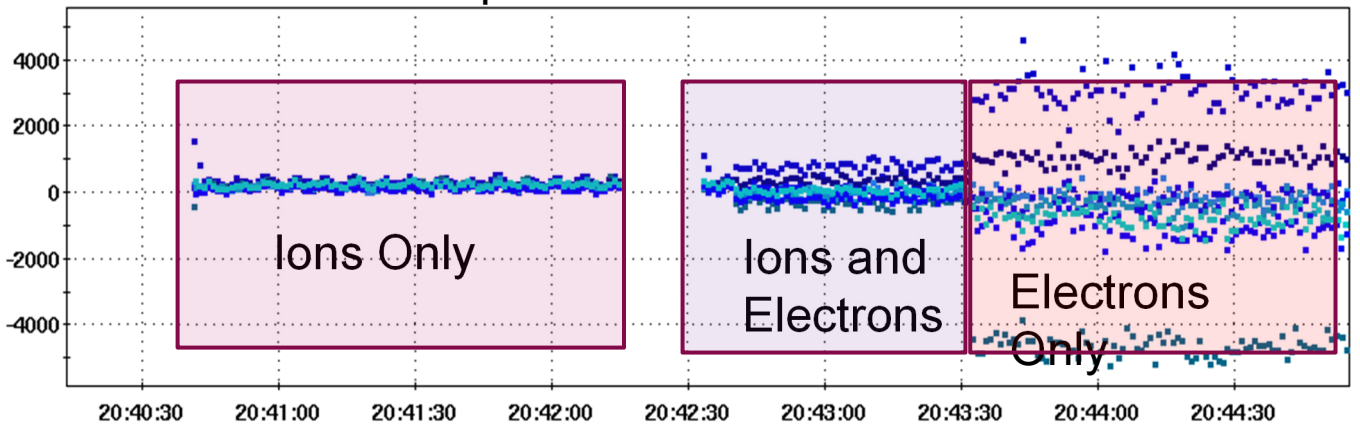

704MHz position – detects only electron beam

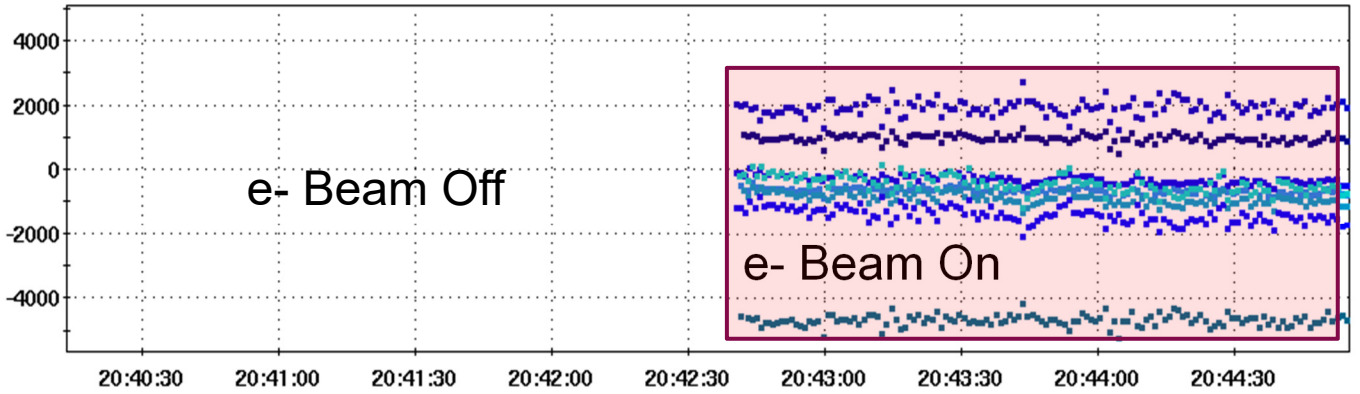

Courtesy R. Hulsart, R. Michnoff

Electron-Ion Trajectory / Energy Overlap: Recombination Monitor

Principle

- portion of fully stripped ions (here, Au) combine, through radiative recombination with electrons in the cooling region
- resultant hydrogen-like ion detected using large-area plastic scintillators at locations with specially-generated large dispersion

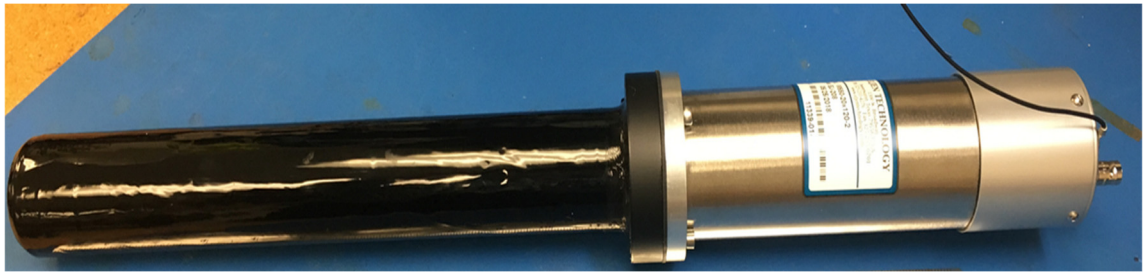

Two modes of operation

- Scaler counter of recombination events
- bunch by bunch monitoring using time digitizers

signal from 6 RHIC ion bunches

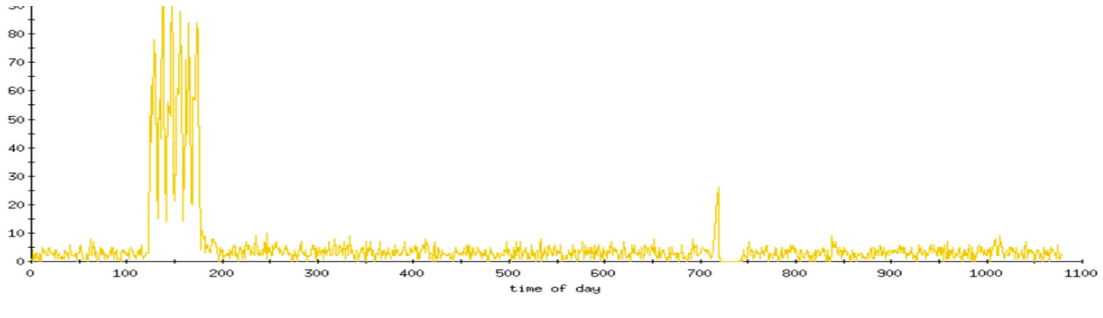

electron-ion energy match achieved with accuracy of ~1 keV (6E-4)

See also T. Miller et al, Overview of the Beam Instrumentation and Commissioning Results from the BNL Low Energy RHIC Electron Cooling Facility, International Beam Instrumentation Conference (2019); Observations of Beam Losses due to Bound-Free Pair Production in a Heavy Ion Collider. Phys. Rev. Lett., 99: 144801 (2007), R. Bruce et al

Electron-Ion Energy Overlap

- RF Voltage – ~100 kV expected (6 – 7%)
- Energy Spectrometer – 6 kV (0.375 %)
  - The spectrometer measurements showed that the initial LEReC settings based on calibration of RF cavities provided about 100 keV different e-beam energy than the design 1.6 MeV energy.
- Recombination Monitor – 1 kV (0.0625%)
  - Also gave confirmation of 180-degree magnet absolute energy measurements system calibration.
- Wall Current Monitor – 100 V (0.00625%)
  - The WCM measured bunch length for longitudinal cooling efficiency for fine tuning of electrons energy (with 100 eV steps)
- Final Cooling Observation – transverse bunch width
  - Fluorescence monitor (CW beam measurements only)
  - IPM (single bunch measurement possible)

wall current monitor

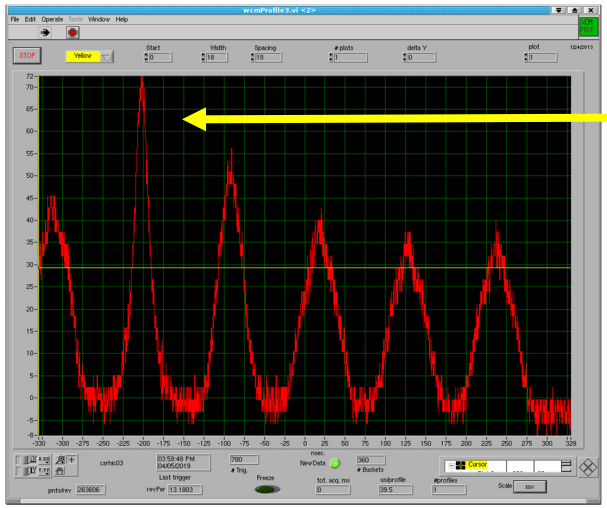

cooled bunch

all other bunches not cooled

bunch length versus time

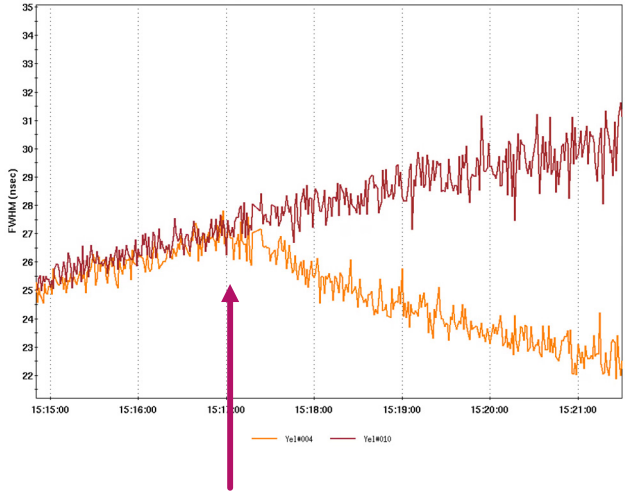

normal bunch

cooled bunch

energy of electrons and ions matched

Electron-Ion Energy Overlap

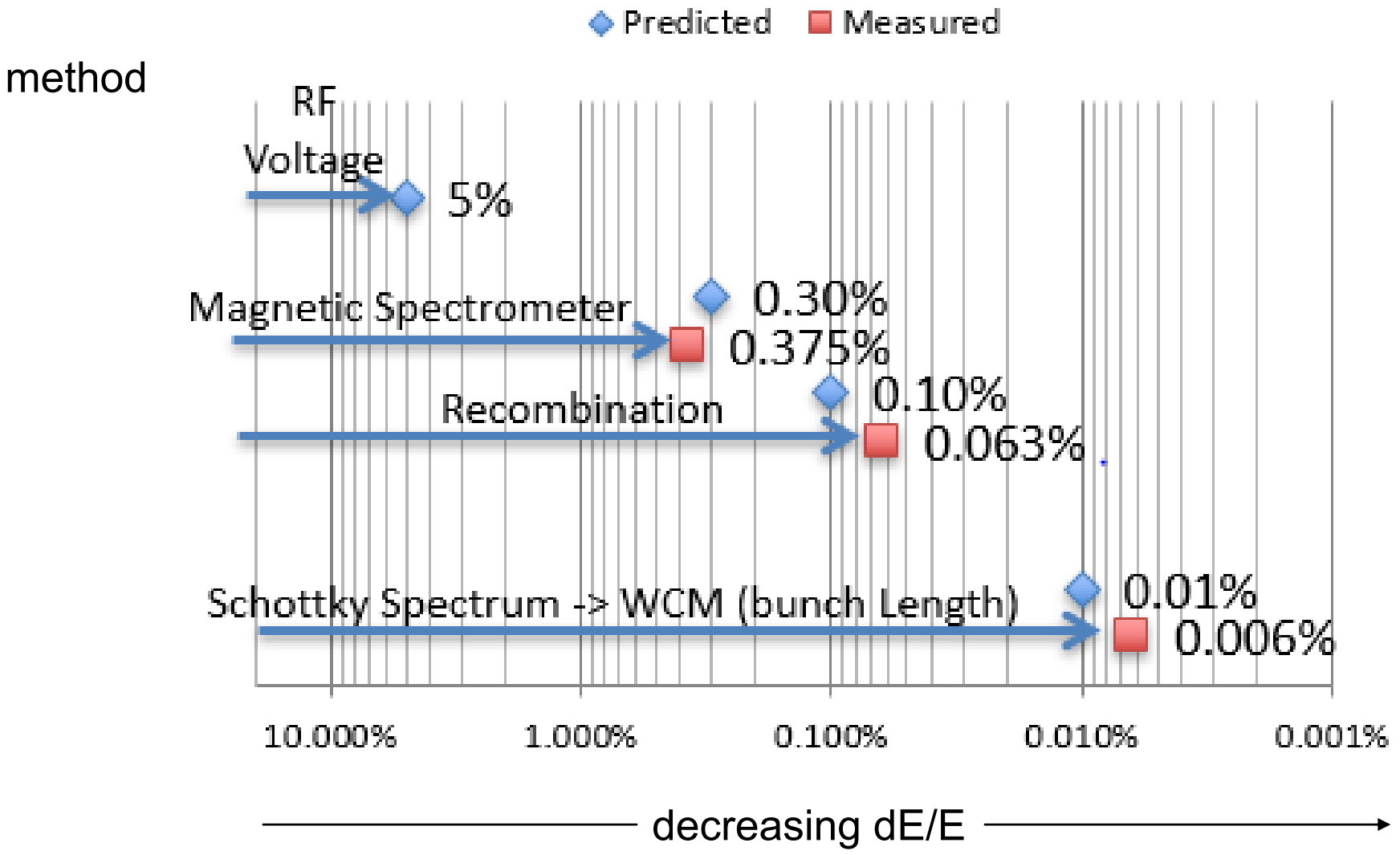

TUZBB3 - Precise Beam Velocity Matching for the Experimental Demonstration of Ion Cooling with a Bunched Electron Beam, S. Seletskiy, et al

Summary

- Beam Instrumentation, select topics reviews (with focus on instrumentation hardware)
- Measurement of Beam Parameters to Characterizing Accelerator Performance
- Presented Recent Developments and their Challenges (with focus on co-propagating beams)


Sponsored by:
APS physics
IEEE
NAPAC2019@frib.msu.edu
www.frib.msu.edu/NAPAC2019
Thank You for your attention!